BLT

Acoustically Triggered Buoyless Lobster Trap Recovery System

Tech 797 UNH Ocean Projects
Engineering Senior Design
1998-1999

Group Members:
Hayden Turner
Jud DeCew
Darryn Goldsmith
Scott Brimlow

Sea Grant
New Hampshire/Maine

Acknowledgments:

A special thanks to:

Ken Baldwin for guidance and a valuable resource.

Robert Champlin for your patience and mechanical wisdom.

John Scott for your help with the budget and all around support.

Laura Cavagnaro with your acoustical expertise.

Adam Perkins for your vast knowledge of electrical components.

Mike Carter as a valuable resource for the electrical engineering.

"This work is the result of research sponsored in part, by the National Sea Grant College Program, NOAA, Department of Commerce, under grant #NA76RG0084 through the University of New Hampshire / University of Maine Sea Grant College Program."

Table of Contents:

List of Figures:

List of Tables:

Abstract (Hayden Turner, Jud DeCew)

The Buoyless Lobster Trap, BLT is an acoustically triggered retrieval mechanism for deep water lobster trawls. The system manipulates a rotary solenoid to discharge a buoy, connected to a line, to the surface from the ocean floor. The electronics, release, and the winding mechanism are the three integrated subsystems which make up the BLT. The design goal was to keep the system simple and use an existing trap as a vehicle for all the components.

The BLT system will replace the current fishing practice indiscernibly. The system will completely eliminate the need for fixed gear which will minimize marine mammal entanglements. The BLT is a simple, robust, inexpensive, and reliable means of accommodating the ALWTRP supplicated by the Department of Commerce. The ALWTRP is the Atlantic Large Whale Take Reduction Plan which requisitions the reduction of mammal fatalities due to commercial fishing practices.

The prototype exploited a Hummingbird Fish Finder to edict as the system transponder which will project the sound wave from the surface vessel to the trap on the ocean floor. The hydrophone was poached from a previous project and the ideal frequency is 160 kilo Hertz. The Hummingbird transmits a signal at 200 kilo Hertz which does not overlap the hydrophone's frequency band so amplification and manipulation of the signal is very inefficient. The final BLT will demand identical sensitivity and operating frequencies of the transponder and hydrophone.

The sea faring portion of the system is made from a converted lobster trap so that handling of traps on deck will not change. Dysfunctional traps are readily available to the fisherman so that the total cost of the system can be reduced. The system hydrophone protrudes out of the trap about two inches due to its origin which creates a stacking problem. The final system will be constructed so that no portion of the system extends beyond the boundaries of the lobster trap. This will protect the contents.

The BLT is a simple device that can be operated by any person, no matter what their background. Simply pressing the button will dispatch the signal and then the rest is analogous to the present lobster trawl hauling technique. Maintenance for the system consists of changing the batteries a couple of times a year. The estimated cost per unit is 315 dollars and each string of traps should have at least two, for safety reasons. These units will replace conventional commercial lobster trawling practices without creating an undue burden to the industry and virtually eliminate the danger to the ever decreasing population of whales.

Background/ Introduction (Hayden Turner, Jud DeCew)

The current technique for lobstering in deep water, up to 1200 ft, is proven to be dangerous to some mammals. The lines run the water column between the traps and the surface buoy, see *figure 1*. The problem with this technique is that marine mammals have become entangled in these lines. A whale's instictive reaction upon brushing up against the line is to roll. When the whale rolls, it entwines itself up in the line and becomes entangled. The entanglement can be fatal for the whale and costly for the fisherman due to damaged or lost or damaged gear.

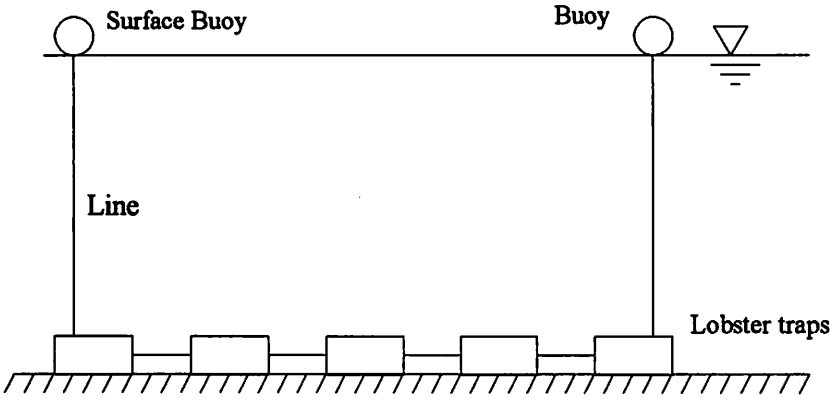

Figure 1: This figure shows the major components and thier relationship to one-another for the current lobstering practices.

The lobster pot lines have entangled humpback, right, and minke whales. The Marine Mammal Protection Act (MMPA) was passed with a long-term goal of reducing the incidental serious injury or lethal take of marine mammals in commercial fishing operations. The Atlantic Large Whale Take Reduction Plan (ALWTRP) asks for an initiation of a gear research and development program into technologies that will reduce the entanglement rate.

Right Whales are particularly susceptible to entanglement due to their migration patterns and feeding behavior which is known as skim feeding. The whales swim slowly at or near the surface with their mouths ajar engulfing the zooplankton. Photographic data indicated 57% of the North Atlantic population has been entangled in fishing gear at some time during their lives (Kraus, 1990).

The Atlantic Large Whale Take Reduction Plan aims to reduce the entanglement without creating an undue burden on the fishing industry. There are several alternate ideas that are currently being researched and tested. Break-away lines, biodegradable lines, and noisy gear are three plausible solutions. Although, each of these has its limitations and don't entirely eliminate the problem. Break away lines still run the water column. This idea incorporates a weak link in the line that breaks if a large force is applied. The link is burly enough to pull the traps from the ocean floor but would be weak enough to fail if a whale should become entangled. This may free the whale, but the gear could also be lost or damaged on the ocean

floor. This results in lost time and money for the lobsterman and doesn't even guarantee the safety of the whales. Another problem is that the lost line could concoct future problems for other marine life. Rough seas or an unexpected force could cause the link to fail.

Biodegradable lines and links are safer to whales because the threat decreases over time. The lines have a weak link, as previously discussed, but also dissolve in water. If a whale became entangled and broke the link, the line wrapped around the whale's body and the lost line would decompose over time. Since the line decomposes in water, the line would have to be replaced after only a few uses. This results in a greater cost for the lobster fishery and in turn for the consumer and a maintenance burden. Initial injuries to the whale while the integrity of the line is still intact could still be devastating.

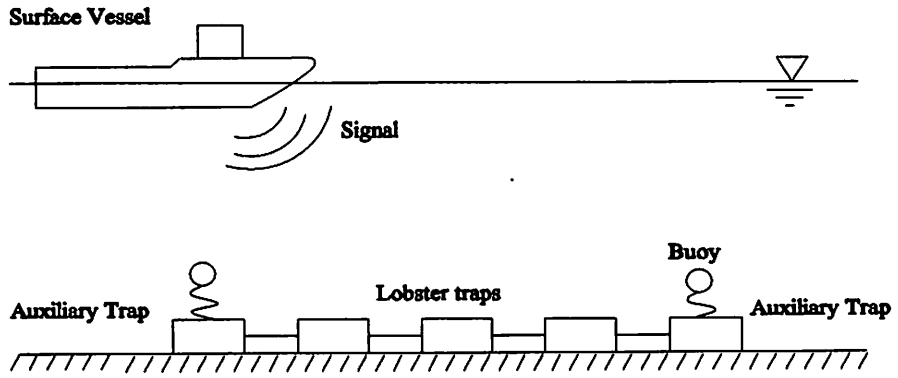

Figure 2: This figure shows the major components and thier relationship to one-another for the proposed acoustically triggered buoyless lobster trap recovery system.

Sound deterrents, "noisy gear",daunts whales with the use sound signals set to a decibel range which whales can hear. Investigation of the effects on other sea life has not been done. The system could attract unwanted creatures to the lines which could create dissimilar problems. Power supplied by batteries to produce these signals can be costly if the signal is constantly broadcasted through the water.

These alternate ideas may look good on paper, but could create an undue burden on the fishing industry. The weak links, biodegradable line, and sound deterrents require more money and time for the lobstermen and won't eliminate the threat to marine life completely. An acoustic release system would have an initial capital investment but would have a low maintenance cost. It would completely eliminate the danger to marine life as well as integrate into the current trapping method. Some time will be lost waiting for retrieval buoy ascend to the surface and changing the batteries a few times a year, but is a viable solution.

The goal of the acoustically triggered buoyless lobster trap recovery system is eliminate entanglements without disrupting current fishing practice or productivity. The system consists of two auxiliary traps connected to each end of the current string (see *figure 2*).

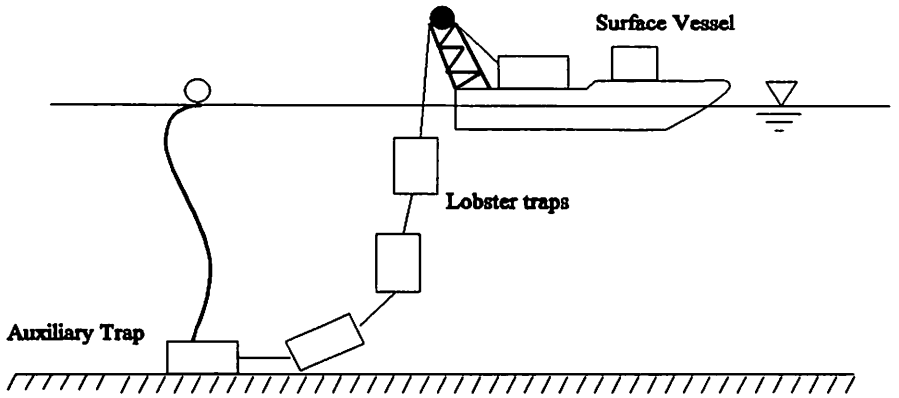

Figure 3: This figure shows the major components and thier relationship to one-another for the proposed acoustically triggered buoyless lobster trap during retrieval.

These unique traps would have a buoy and line confined within the safety of the housing. When the surface vessel approaches, it conveys an acoustic signal to the trap which is received by a hydro-phone. The auxiliary trap will release the buoy which is attached to a retrieval line. The auxiliary trap and the attached lobster pots can then be hauled up with this line using the same techniques currently in use, see *figure 3.* By eliminating the lines in the water column except during the short retrieval of the gear, the endangerment to marine animals will be minimal.

Alternate Releases (Hayden Turner, Jud DeCew)

Several viable releases were examined before the final decision on the solenoid and key release was finalized. All of these releases use an acoustic signal to initiate the release of the buoy. The releases have certain criteria they must satisfy; which are:

1. Simple
2. Minimum amount of moving
3. Corrosion resistant
4. Deter biological growth.
5. Durable
6. Battery powered and efficient

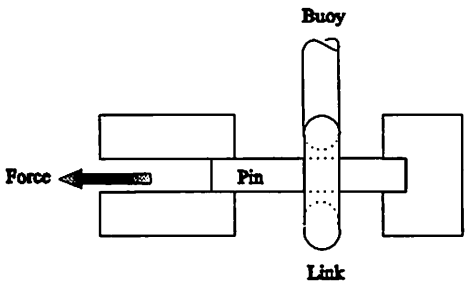

Figure 4: Release I

The first release can be seen in *figure 4.* The pin would be moved by a force generated by an electromagnet or linear solenoid. The link around this pin prevents the buoy from rising prior to activation. Once the signal is received, the electromagnet pulls the pin out which allows the buoy to rise to the surface.

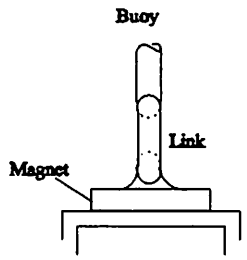

Figure 5: Release II

The advantage of release I is it's simplicity and has few moving parts. Some of the disadvantages include the large frictional force between the pin and the link. Any biological growth on the release could inhibit the movement of the parts. Also, the electromagnet would have to supply a large force to overcome the friction within the channel in which the pin slides.

Release II uses an electromagnet to restrain the buoy until the signal is received. The current flowing through the wires that created the magnetic force would terminate when the signal arrives. The unrestrained buoy will be able to rise to the surface. *Figure 5* displays this idea.

The advantages of this design are that there are no moving parts and biological growth would not prevent the mechanism from operating correctly. If the power supply deceases, the buoy would be released thus saving the gear. One disadvantage would be the large force needed between the magnets to bulwark the buoy. The magnet would also require a constant supply of current to keep the buoy arrest.

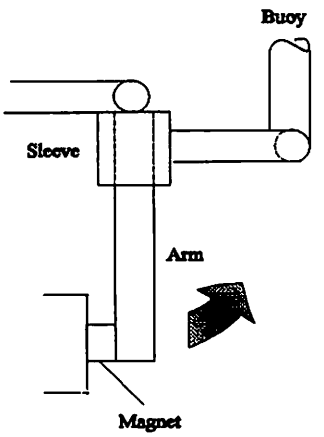

Figure 6: Release III

The next design was a hybrid of the first two; which will decrease the magnetic force and the frictional forces as shown in *figure 6*. When the signal is received, the magnet will release the arm. The arm will then rotate 180 degrees, and the sleeve will slide off.

The main advantage to this type of release is the decreased force required by the magnet. A few reasons for not using this type of release include the number of moving parts. The pivot point could get obstructed by foreign matter and prevent the arm from rotating the full 180 degrees. There is still a significant power drain associated with the electromagnet.

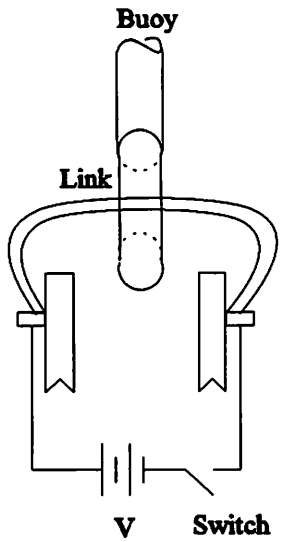

Figure 7: Release IV

These are the designs that make use of a magnet in the release system. In general, these releases were not considered for the final design due to their constant current requirements. Some other designs using magnets were discussed but only a few appear in the report.

Other possible designs incorporated a filament which would burn out as high current passed through it. *Figure 7* displays a sketch of the filament release mechanism. When the system is activated, the switch closes the circuit and current begins to flow. The filament would then melt due to heat produced while the high current passed through a small wire

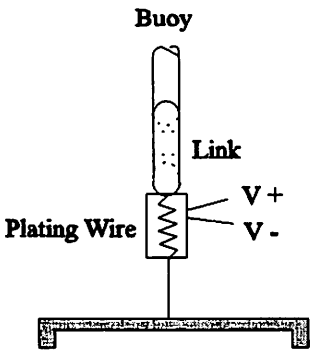

Figure 8: Release V

with a low melting point. The buoy would then break free and ascend to the surface. Biological growth would not affect this design as it would in previous release ideas, and again it is simple with no moving parts. But, the filament would require an ample supply of current and the filament would very likely be brittle at 4 degrees Celsius. The filament would also have to be replaced after every use and seawater is fairly conductive which could hamper the release from operating effectively.

Wire runs through a small cylinder filled with seawater. The water is charged with a small current, melting or plating the wire inside the cylinder away, see *figure 8*. The wire decays until the buoyant force exceeds the tensile strength of the remaining wire and then the buoy discharges. The advantages are that the current needed to degrade the wire is only 300 mA. It is simple with no moving parts. One large disadvantage is the cost of such a release. The wire release is costly and has a one time use. Also, it takes approximately 15 minutes to degrade the wires. This translates into more waiting for the lobster men and time is money.

Release VI can be seen in *figure 9*. An exploding bolt appears to be a regular bolt with a fuse and small explosive charge placed inside. When the signal is received by the hydro phone, a current is sent to the fuse and the bolt explodes. The arm would be made of buoyant material so it would rise out of the buoy's path.

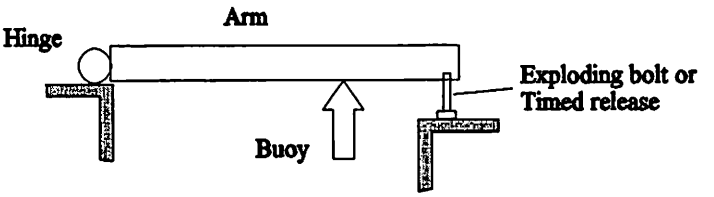

Figure 9: Release VI

This design has very few moving parts, but the one time cost of each bolt is far too expensive. The smallest and least expensive exploding bolt costs $200. It can hold 1500 lbs, 50 lbs buoyancy, which is far greater than any force expected. The bolts would have to be changed after every use and can be very dangerous to the installer. This release is far too costly to even be considered for the final design.

Galvanic timed releases were also researched. The set up of the release mechanism is shown in *figure 9*. Galvanic timed releases decompose in seawater. The water slowly breaks down the surface layers until the tensile strength of the release is insufficient to withhold the buoyant force. The releases can be purchased to accommodate any time frame desired. They have to be changed after each use but are cost effective at $3 a piece. The main disadvantage of this timed release is that the operator of the boat has no control over the release. No signal is needed, and the release will only go off after a specified time. The lobster men can not retrieve the lobster pots earlier than the release will allow. If he or she attempts to recapture the traps later than the designated time release then the buoy will be sitting on surface with

the line in the water column. The line would then pose a threat to the marine life which is what this system attempts to eliminate. Since weather cannot always be predicted accurately, these releases will be eliminated from the running even though they are the cheapest thus far.

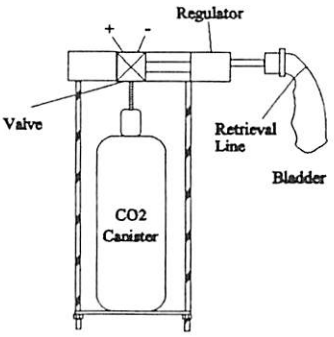

Figure 10: Release VII

The next design idea embodied an inflatable buoy. This design employs a bladder filled with CO_2. A signal received from the surface will trigger a valve which would allow the bladder to fill with CO_2 gas from a canister and float to the surface. *Figure 10* displays the release idea.

Biological growth would have little effect on this design and there are few moving parts which could produce a failure. Some problems with this design include the bladder undergoing drastic volume changes during its ascent through the water column. The bladder would require an extremely high initial pressure to initiate the system. It could also over inflate and rupture when encountering the drastic volume changes through the water column. The CO_2 canister would also have to be replaced frequently.

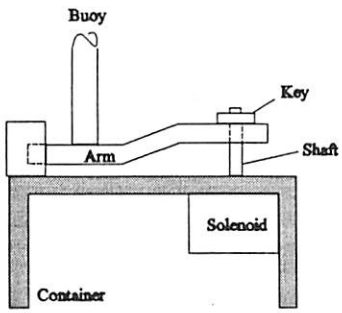

Figure 11: Release VIII

Release VIII is most comparable to the final design choice where a rotary solenoid is housed inside a water tight container. Protruding out of the container will be a shaft turned by the solenoid actuator. This will rotate a key between 45 and 90 degrees to fit through a slot on the arm. The buoy will pull the arm free and approach the surface. *Figure 11* shows the configuration of the parts described above. A distinct advantage to the design is easy reloading and is reusable.

The arm attached to the buoy by a leash will travel with the buoy to avoid entanglement of the line. One of the major drawbacks to this design is an increased cost caused by the complexity of parts to be machined. A seal around the shaft will have to be watertight to 650 psi to protect the electronics inside of the container. Any holes in the container could create potential problems because the electronics will cease to function in saltwater. The arm will have to be supported laterally to prevent it from sliding around as well as to ensure that the key and the slot will line up correctly.

This type of design proved to be most feasible because of its initial capital investment and low long term costs, low maintenance, and ease of use. A canister must be machined to accommodate the electronics in each prospective design, so this canister could be made to be slightly larger to make room for the solenoid. Reloading is simple to do; intrusion into the canister only needs to be done a few times a year to change the batteries.

Final Design Approach (Hayden Turner, Jud DeCew, Darryn Goldsmith)

The final design of the robust acoustic release system was based on overall cost, simplicity, and effectiveness of solving the problem at hand. The entire system can be broken down into three subsystems; the first and most crucial is the mechanical release, then the electronics and acoustics, and finally the rewinding system, see *Appendix E.*

Release (Hayden Turner, Jud DeCew)

A solenoid actuator was picked to trigger the release because it is commonly used on other acoustic release systems. A rotary solenoid was chosen because of its simple design and its low power consumption. It has a spring induced holding torque which can be utilized to retain a key with no power consumption. A rotary solenoid uses a ramp to convert a linear motion into a rotational motion see *figure 12.* The solenoid will be used to turn the key.

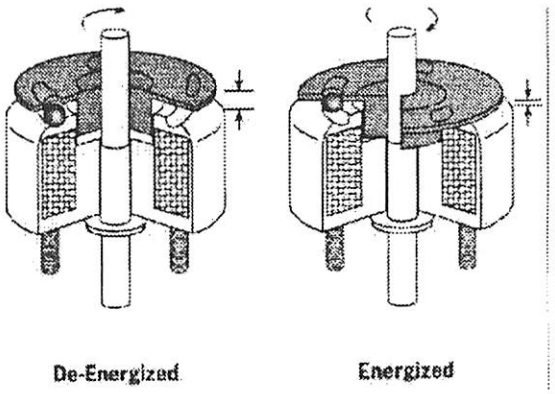

Figure 12: Shows how a rotary solenoid converts a linear motion into a rotational motion through the use of a ramp.

The key is simply a rectangular box made a white delrin which has chamfer on all sides. White delrin is a water lubricated plastic that has a very low coefficient of friction and resists biological growth. It can be machined easily and is also durable. The key will fit through a rectangular opening in a retaining arm that will restrain the buoy. The key will be mounted on a quarter inch stainless steel shaft and then connected to the rotary solenoid with a quarter inch shaft coupling.

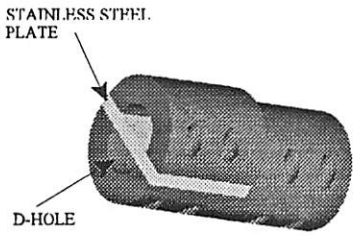

Figure 13: This shows the coupling in detail.

The coupling has to mount statically to the solenoid but allow some vertical movement due to the nature of the rotary solenoid. The solenoid uses a ramp to convert a linear motion to a rotary motion. The total vertical displacement is only about an eighth of an inch but must be accounted for when dealing with high pressure seals. Any linear movement within the seal will cause a leak which could be devastating. To eliminate the possibility of a leak the shaft is constrained using a D shape on the end of the shaft where it meets the coupling. A small piece of stainless steel that is one sixteenth of an inch thick was placed between half the coupling. The steel plate separates the normal circular hole in the coupling to two D shaped holes, shown in *figure 13.* This design will allow the shaft to slip in the vertical direction but will still be restrained in the radial direction.

The shaft is made of stainless steel and is held in place by the coupling, a retaining E clip, and a rulon flange bearing. The shaft has a diameter of one quarter inch to keep the moment of inertia to a minimum. Minimizing the moment of inertia will enable the solenoid to accomplish its ultimate goal unhampered by the bulk of an oversized shaft. The retaining clip simply restrains the shaft from

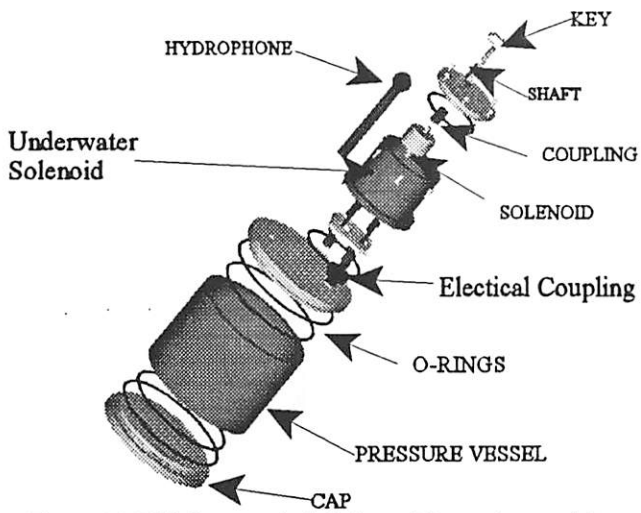

Figure 14: This is an exploded view of the canister and the underwater solenoid.

moving in the vertical direction within the solenoid canister.

The main canister in the release system is the larger of the two pressure vessels shown in *figure 14.* This is where the electronics will be contained and protected from the ocean water. The canister itself can be seen in *appendix F.* The pressure vessel has a wall thickness of a half inch thick and height of six inches. This size was chosen based on the materials at our disposal. The canister is based on several pre-existing pressure vessels that are currently in use for ocean research at the Jerry Chase Ocean Engineering Laboratory at the University of New Hampshire.

The internal volume of this particular canister was larger than needed but the original design required that the rotary solenoid be housed within this pressure vessel. The vessel had to be large enough to hold eight D cell batteries, an electronic bread board, and a processor which would demodulate signals received by the hydro phone. The solenoid was excluded from this canister due to difficulties encountered while searching for dynamic seals that can withstand a pressure of 600 psi during 45 degrees of rotation. Most of the seals used for deep sea applications are manufactured by a few select ocean engineering companies. They will make custom seals for a specific application but request either large sums of money in return or minimum purchase of a thousand units.

The pressure vessel caps were machined out of T6 aluminum alloy. The plates are one inch thick and each has two o-rings to prevent water from entering the canister. This will further minimize the risk of a leak which cannot be tolerated, especially when the pressure vessel is to be filled with expensive electronics. The caps will be fastened to the pressure vessel by six compression spring latches, three for each cap. This will allow easy access to the container to change the batteries.

An underwater solenoid was designed and fabricated which can be seen in *figure 14.* The underwater solenoid consists of the upper canister and all of the internal and external components shown in *figure 14.* The underwater solenoid is attached to the pressure vessel. The canister was made out of T6 aluminum alloy and attached to the pressure vessel by six 8-32X1/2 inch cap screws. An o-ring was placed between the two faces to prevent any oil and water mixing at the base. A watertight electrical connector transmits electrical power from the battery pack in the pressure vessel to the solenoid. The solenoid chamber is filled with a non-conductive incompressible fluid which relieves the dynamic sealing problem. Vegetable oil will be used for the prototype because of its accessability.

The solenoid can cap has one o-ring on the inner mating surface. The o-ring functions as both a piston and a barrier between the seawater and the oil. Once the canister is filled with oil, pressing the

cap into place will cause excess oil and any air bubbles to be forced out of the small area between the shaft and the rulon flange bearing. Once this is done then the cap should be wiped clean and the lip seal pushed down firmly until it comes into contact with the bearing. This will create a tight seal that will prevent any leaks. The cap was made of T6 aluminum alloy and is attached by six 8-32X1/2 inch cap screws.

The retaining arm is held in place by the key on one side and by a bracket on the other. The bracket simply prevents the retaining arm from getting knocked off by accident and keep it in the proper position. The arm is made of white delrin and has a key-way cut into it which is slightly larger than the key itself. The arm will have a leash attached to it to avoid losing it on the ocean floor.

Electronics: (Darryn Goldsmith)

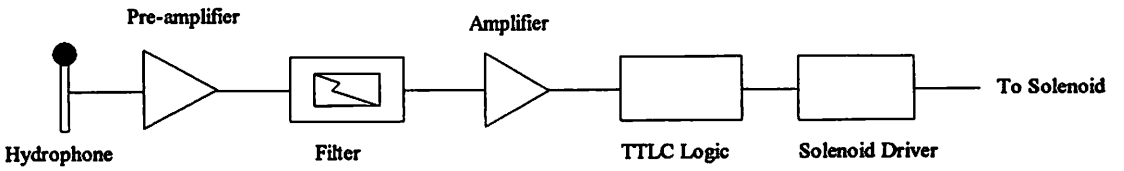

Figure 15: Block Diagram of electrical components.

The signal source used with the prototype design was a fish finder. The incoming signal to the hydrophone will be amplified and filtered to eliminate extraneous noise, see *figure 15*. The signal remaining in the desired bandwidth will then be amplified again and passed to the logic circuit where it will lock on to the recognized frequency of the fish finder. This will initiate the logic block to turn on the power transistor, which in turn activates the solenoid.

There are two main approaches to solving this problem. The first is using discrete components with no frequency recognition. The second approach is to combine integrated circuits with discrete components. The first approach involved the use of discrete circuit components and was considered for several reasons. A design using individual parts can be separated and recombined providing maximum flexibility. Modules can be created that perform specific functions and in turn can be repositioned within the overall system. This allows the designer the freedom to move functional components to wherever they are needed. For example, if a gain stage performs poorly or is no longer needed it can be removed and replaced just by disconnecting the module. In addition, entire modules can be interchanged with one another in many configurations. The designer could observe how well the system works, with or without any module, and could implement these changes on site. Unlike integrated circuits, a discrete modular design could significantly reduce the downtime should an unforeseen problem occur.

An integrated circuit also has many benefits that outweigh some of its limitations. First and foremost, ICs are small and cheap. One IC can perform many functions using small amounts of space when compared to the impractical size and singular functionality of a discrete module. For the purchase price of one discrete component an IC package can often be bought at a fraction of that cost. They are also fast, reliable, and require much smaller power supplies than discrete components.

Because the sending station of our link to the traps operates at a high frequency, as well as a low pulse width, a combination of integrated circuitry and discrete components was chosen. The ICs will take care of the signal reception and initiate the appropriate logic signal while the discrete components will drive the solenoid to release the float.

The circuit board itself has not been set for testing. Salvaged parts from previous projects will be incorporated with the new devices and will be working by May 11th.

Winding System (Hayden Turner)

The winding system is used to rewind the line on board the ship once the lobster traps have been recovered, see *figure 16.* It is simply a belt driven pulley system that gives the person winding the line an advantage of 5:2 so for every two revolutions of the winding gear the spool makes five. This will expedite the winding process.

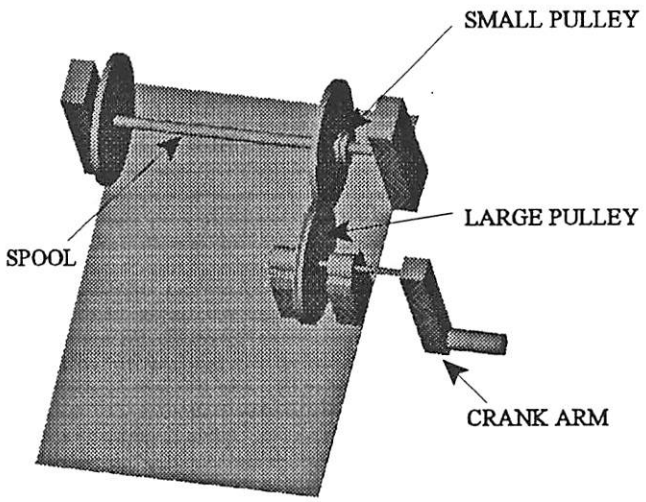

Figure 16: This figure shows a simplified representaion of the winding system.

Once the line is wound onto the spool, the trap will be ready to be armed. The pulley system is disengaged by removing the belt from the pulley. The belt has just enough tension to avoid slipping and still be easily removed. This will allow the spool to spin freely on the ocean floor as the buoys ascent to the surface. The crank arm also detaches from the major drive pulley when the winding is finished. The crank arm is fastened to the large pulley through the use of a threaded coupling.

The spool is a one inch diameter aluminum bar spanned between two delrin flange mount bearings. Two eleven-inch diameter plywood plates, held there by flange shaft mounts, keep the rope in the designated area. The small pulley is fixed to the shaft so that the entire spool will spin in the winding mode. The spool was designed to decrease the possibility of entanglement of the retrieval line by coercing a predictable escape. If the line were placed into the trap haphazardly there would be no envisioning of how it would exit.

Design Verification (Hayden Turner, Jud DeCew)

Buoy Analysis Using A Depth Step Approach (Jud DeCew)

An integral part of the BLT system is the buoy itself. It is important to determine the rising velocity, the time it takes to reach the surface, and the size of the buoy needed. The lobstermen at the surface need to know how long of a wait to expect before the buoy surfaces and more importantly if there is a malfunction. The analysis was approached using two methods. The first was a depth step approach. Several assumptions were made to simplify the analysis. The water was assumed to have constant density and viscosity. The system is modeled for the worst case scenario, where the density and viscosity are assumed to be equal to that at 1200 feet. Secondly, the buoy is a spherical and radial deflections of the buoy were considered to be negligible and could be ignored. This implies that the buoyant force is constant. The line attached to the buoy is considered to be neutrally buoyant which is also known as "floating line."

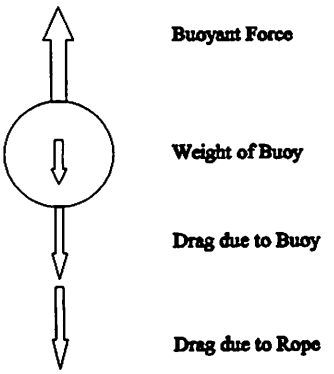

Figure 17: Free Body Diagram of the rising body

A body rising through a fluid has multiple forces acting upon it. There is the buoyant force of the body. Acting against the buoyant force is the weight of the body, the drag of the water around the body, and the drag of the line, which the body is lifting. *Figure 17* displays a free body diagram of the rising buoy.

Equation 1 shows the sum of the forces from the free body diagram.

$$F = F_{buoyant} + W_{buoy} + D_{buoy} + D_{rope} \quad [1]$$

where $F_{buoyant}$ is the buoyant force, W_{buoy} is the weight of the buoy, D_{buoy} is the drag of the buoy, and D_{rope} is the drag of the rope. The acceleration of the buoy can be found by using equation 2.

$$a = \frac{F_{buoyant} + W_{buoy} + D_{buoy} + D_{rope}}{m} \quad [2]$$

The equations for the forces can be found in the *appendix A* as well as a full description of the analysis. It is important to note that the drag force created by the buoy is dependant upon velocity. Also, the drag force of the line is dependent upon both the velocity and surface area of the line. *Equation 3* describes the relationship between the drag and velocity. As the buoy rises, the rope's surface area increases linearly with the length of the rope therefore, increasing the drag. *Equation 4* describes the relation between the changing surface area and the length.

$$D_{rope}(V, L) = \frac{1}{2} \cdot \rho \cdot V^2 \cdot S_s(L) \cdot C_d \quad [3]$$

$$S_s(L) = 2 \cdot \pi \cdot r_{rope} \cdot L \qquad [4]$$

where r_{rope} is the radius of the rope, V is the velocity, g is the gravity constant, ρ is the density of the fluid, S_s is the surface area of the line, L is the length of the rope, ρ is the density, and C_d is the drag coefficient of the line.

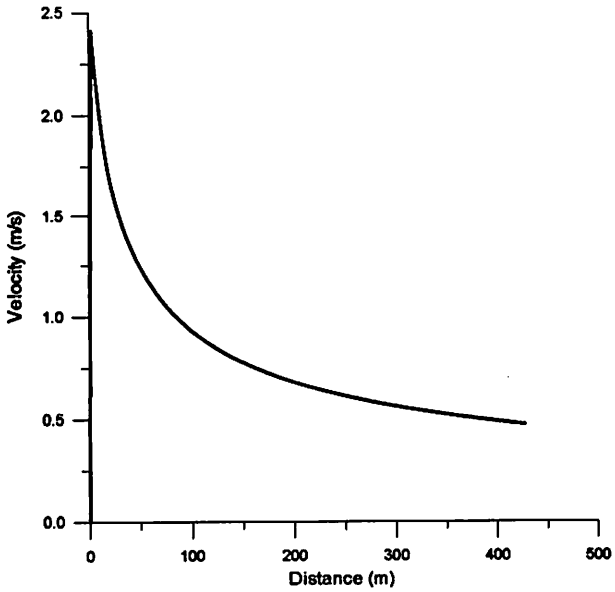

Figure 18: This plot shows the velocity versus distance

The depth step analysis was approached by breaking up the distance the buoy has to travel into one meter increments. Then the buoy is analyzed at each of these depths by recalculating the forces using the average velocity from the proceeding section. For this analysis to work, first assume the acceleration of the rising buoy is zero. In the "real world" the acceleration would be negative as the buoy slows with an increase of drag, but because the acceleration change is so small over the set distance it can be neglected. Attempting to run the simulation considering the change in the acceleration resulted in a singularity because the acceleration became infinitesimally small. This model is based on the principal of virtual work. If the acceleration is zero then the simulation simply recalculates the terminal velocity after each step. The results of this analysis can be seen in the *appendix A.*

Using the velocity and the distance traveled, the time to reach the surface can be calculated. It is important to note that the buoy never reaches a true terminal velocity but very slowly decreases in velocity due to the drag of the rope.

Figure 18 displays the velocity versus distance for the rising buoy. The distance traveled is 1200-ft (426 m) which is the approximate depth the lobster trap system will be deployed. A graph of the drag of the rope versus distance is shown below in *figure 19.*
The drag is linearly related to the distance because the drag increases as more line enters the water column. With the use of buoyant line the significant force is due to drag.

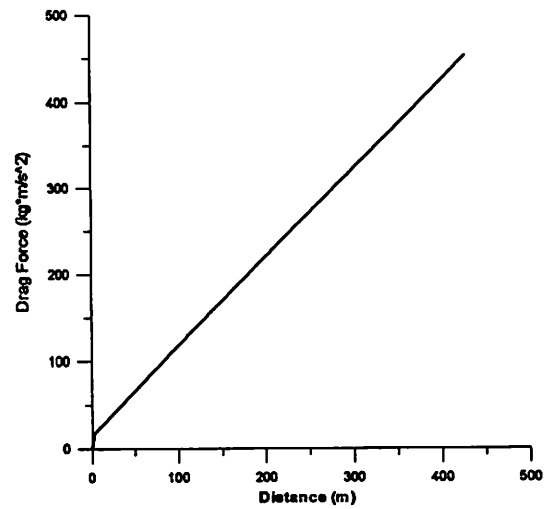

Figure 19: This plot show the drag force over the distance.

A major concern is the coefficient of drag for the rope.
This value is difficult to determine and can greatly change the outcome of the analysis. The rope is traveling through the water column and creates a boundary layer of static water molecules at the contact surface. The coefficient used is based on empirical data and the exact value could not be determined. *Table 1* displays some numbers used and the resulting data obtained.

Table 1: Data and results obtained.

Properties	SI Units	English Units
Density of fluid	1027.7 kg/m^3	64.157 lb/ft^3
Kinematic viscosity	1.6094 x 10^{-6} m^3/kg	2.578 x 10^{-5} ft^3/lb
Dynamic viscosity	1.08 x 10^{-3} m^3/kg	0.017 ft^3/lb
Radius of the buoy	.152 m	.5 ft
Rope Diameter	6.35 x 10^{-3} m	.25 in
C_d (buoy)	.1	.1
C_d (rope)	.05	.05
Gravity	9.81 m/sec^2	32.2 ft/sec^2
Volume of buoy	.0144 m^3	.508 ft^3
Distance traveled	426.7 m	1200 ft
Peak Velocity	2.33 m/sec	7.644 ft/sec
Time to reach surface	10.3 min	10.3 min

Buoy Analysis Using A Time Step Approach (Hayden Turner)

Another model was created using a similar approach and assumptions. The model does in fact account for the acceleration of the buoy. The full procedure can be seen in *appendix B.* The equations of motion were solved for the acceleration of the buoy and put into state variable form. Euler integration was used to solve the differential equations numerically over time in MathCad.

The rope drag force was modeled as a flat plat which may be conceptually hard to understand. If it were possible to slice the rope along the length and lie it out flat on the surface it could be considered a flat surface. Another way to look at it would be to take a piece of paper and roll it up into a cylinder. A boundary layer at the surface of the flat plate can be estimated using Reynolds Number which is a function of both velocity and length. Reynolds number is shown in *equation 5;*

$$\mathrm{Re}_L = \frac{q_2 * q_1}{\upsilon} \qquad [5]$$

where the velocity and position are in state variable form:

q_1 is the position

q_2 is the velocity

υ is the kinematic viscosity

The drag coefficient for the rope is a function of the Reynolds number so that when the flow begins to become turbulent the drag increases non-linearly. The model accounts for the acceleration of the buoy over 0.1 second time steps. Each iteration recalculates the terminal velocity but will only use the previous estimation for the velocity if the acceleration becomes negative. The results of this analysis can be seen in *figures 20 and 21.*

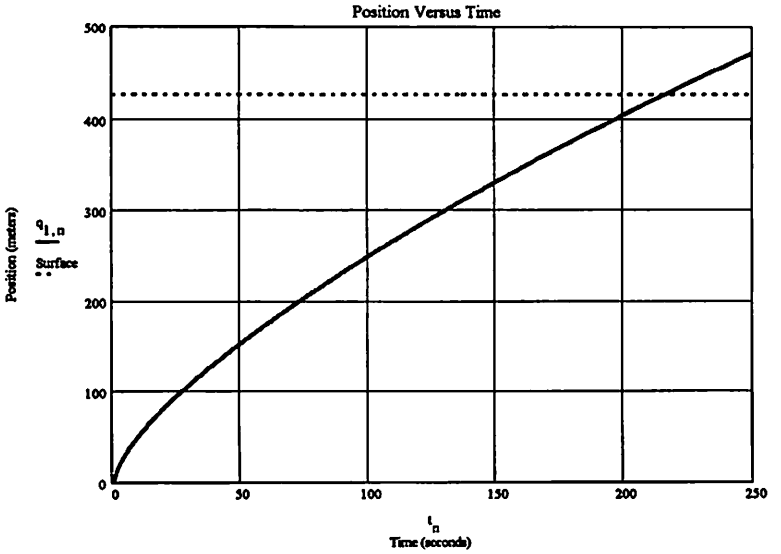

Figure 20: This plot shows the position versus time where the dotted line indicates the surface.

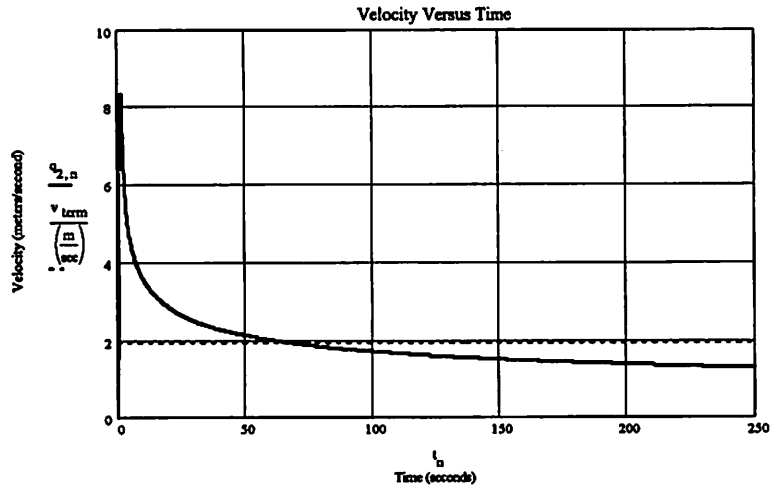

Figure 21: This plot shows the velocity of the buoy as a function of time, the dotted line is the average.

The important results of this analysis are shown below in *table 2.*

Table 2: These are the results of the buoy analysis using a time step approach.

Properties	SI Units	English Units
Density of fluid	1027.7 kg/m^3	64.157 lb/ft^3
Kinematic viscosity	1.6094×10^{-6} m^3/kg	2.578×10^{-5} ft^3/lb
Dynamic viscosity	1.08×10^{-3} m^3/kg	0.017 ft^3/lb
Radius of the buoy	.102 m	4 in
Rope Diameter	6.35×10^{-3} m	.25 in
Gravity	9.81 m/sec^2	32.2 ft/sec^2
Volume of buoy	.0044 m^3	268 in^3
Distance traveled	426.7 m	1200 ft
Average Velocity	1.957 m/sec	6.421 ft/sec
Time to reach surface	3.63 min	3.63 min

Seal Testing (Jud DeCew)

Testing of the seals was conducted in hyper baric chamber located in the Jerry Chase Oceanography Research Laboratory. The canisters were submerged in bucket of water and placed in the hyper baric chamber. A pressure was applied to the system equivalent to a depth of 150 feet. The seal held fast and did not permit any water to penetrate into the internal regions of the containers.

Orientation Testing (Hayden Turner)

A crucial part of the entire system is that it will land on the ocean floor with the proper orientation. The system was tested by throwing the trap into the Oceanography tank which has a depth of 20 feet. The system was initially unbalanced and more buoyant at one end. Initially the load was balanced by extra buoyancy placed on the spool side of the trap, but the trap became totally buoyant and would not sink. Then two bricks were strategically placed on the buoy end of the trap to offset the buoyancy of the buoy. The system now lands with the correct orientation each and every time no matter which way it is thrown into the tank. This is crucial to the operation of system.

Release Testing: (Hayden Turner, Jud DeCew)

The mechanical system of the BLT was tested in the Engineering Tank. A waterproof wire was run from the container to the surface where a power supply was present. Initially, when the power was on, the buoy was not released. This was caused by misalignment of the keyhole and the key. After slight modifications, the buoy released with ease. This was imperative to ensure the mechanical system operated correctly.

Finite Element Analysis: (Jud DeCew)

A watertight container is needed to protect the electronic equipment in 1200 feet of water. The container must be examined for possible modes of failure. This container will be modeled to investigate the deflections and stresses of the canister. Applying a uniform pressure over the entire external surface of the container and analyzing the results will help determine the wall thickness needed. Testing the container for its strength and durability can be done by varying the material and thickness.

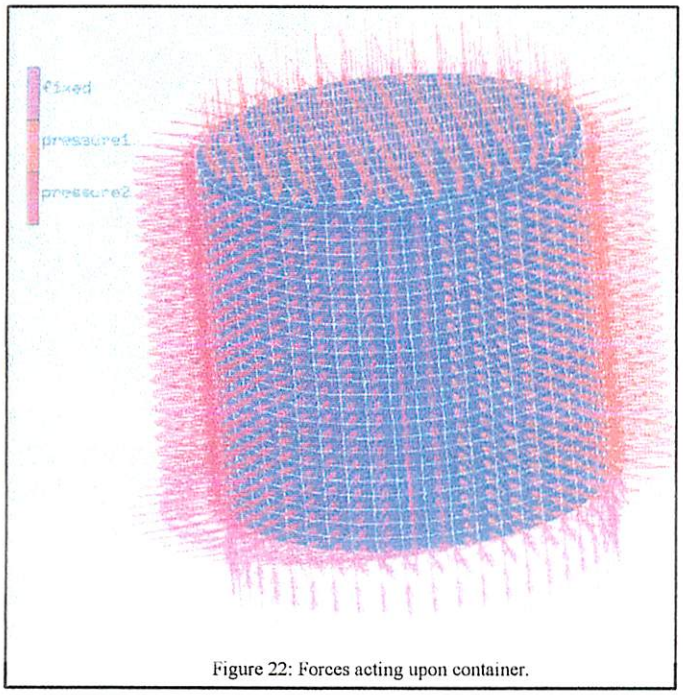

Figure 22: Forces acting upon container.

The analysis of the canister was accomplished using a three-dimensional modeling program called Marc Mentat. A shell was designed for the dimensions of the container: six inches long with an eight-inch diameter. The final result was a hollow shell with a cap at one end, consisting of 1,312 elements.

The bottom of the container was fixed. In the program, some portion of the model must be fixed so forces can act against it. All six degrees of freedom were fixed along the bottom edge of the container. A pressure of 670 psi was placed on every face of the model, see *figure 22*. This simulated the water pressure that would be encountered at a depth of about 1,500 ft. This excess depth is for safety in case the lobster trap exceeds 1,200 ft. In *figure 22*, there are two forces present; the pressure forces are 670 psi and the fixed forces. The fixed forces do not apply any force but hold the shell in place.

Aluminum and steel were considered for the canister material. Aluminum is lighter, more resistant to corrosion, cheaper to machine, but more expensive. Steel is heavier and costly to machine but less expensive. *Table 3* displays the material properties for steel and aluminum. These properties were used in Marc Mentat program model of the canister.

Table 3: Physical properties of materials considered in FEM of Container.

Material	Young's Modulus	Poisson's Ratio
Steel	30 x 10	.292
Aluminum	10.5 x 10	.334

.The thickness of material was picked by perusing the resources available in the school machine shop. Tubes with a thickness of a half inch could easily be obtained for each material. This initial thickness was used in the analysis. The displacements of the steel and aluminum can be seen in *Table 4*. The negative displacements simply indicate that the container is in compression. It is important to note that the X-Y plane is perpendicular to the long end of the container. Perpendicular to the top of the container is the Z-plane.

Table 4: Displacements in the container of aluminum and steel.

Material	Maximum X-Y Displacements	Maximum Z Displacement
Aluminum	-0.001196 in	-0.01351 in
Steel	-0.000418 in	-0.00479 in

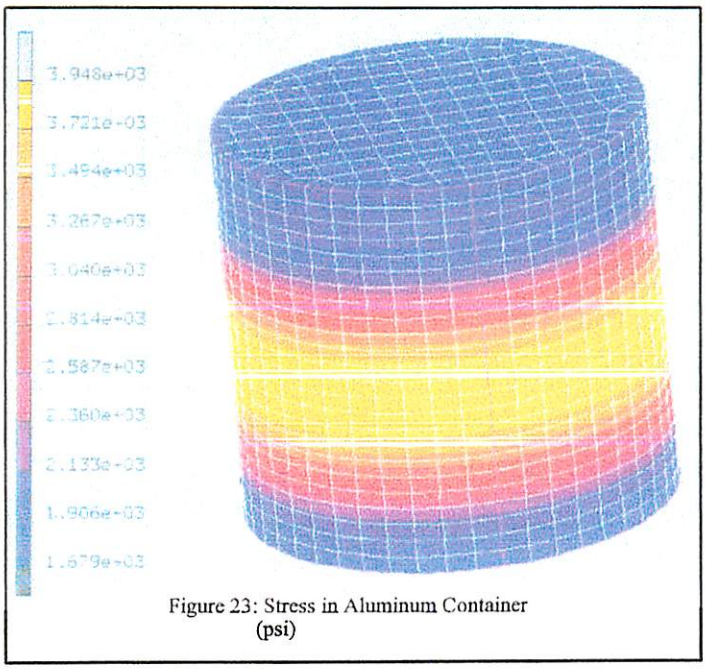

Figure 23: Stress in Aluminum Container (psi)

Neither material had large displacements in a half inch thick container. The steel was displaced less than the aluminum in both planes. The stresses were analyzed next. In Marc Mentat, equivalent stress was used. This is the same as yielding stress in the structure. *Figure 23* shows the output of the aluminum container.

The highest stress concentration occurred in the middle where it is furthest from the support of the caps. The stress is symmetrical around the circumference of the container. This is to be expected, and thus helps verify the data from Marc Mentat.

According to the model, neither the aluminum nor steel failed at this pressure. They experienced the same stress, as would be expected under identical conditions. The steel has a higher safety factor due to the higher yielding strength of the material. *Table 5* displays the results from the analysis of both materials.

Aluminum was the final material choice due to its higher resistance to corrosion than the steel and availability. Although the steel is stronger and has a higher yielding point, the aluminum's performance is sufficient for the pressures expected to be encountered by the BLT system. A safety factor used for the aluminum will compensate for any extra pressure that may be applied to the canister.

Table 5: Stress in Aluminum and Steel Container.

Material	Yield Stress in Container	σ_{yield} for Material
Aluminum	3946.17 psi	35,000 psi
Steel	3950.67 psi	45,000 psi

Thick Walled Cylinder Analysis: (Hayden Turner)

The canister was modeled as a thick walled cylinder to account for subtle differences between the actual canister and the FEM model. Some of the differences are that the caps are one inch thick and the canister is not a rigid container. The FEM model assumes that the cap is welded to the canister or the entire container is one rigid piece of metal that is a half inch thick. The thick walled cylinder calculates the stresses in the container for the tangential and radial directions. The two equations can be seen below.

$$\sigma_t = \frac{P_i r_i^2 - P_o r_o^2 - r_i^2 r_o^2 \frac{P_o - P_i}{r^2}}{r_o^2 - r_i^2} \quad [6]$$

$$\sigma_r = \frac{P_i r_i^2 - P_o r_o^2 + r_i^2 r_o^2 \frac{P_o - P_i}{r^2}}{r_o^2 - r_i^2} \quad [7]$$

where;

σ_t is the tangential stress
σ_r is the radial stress
P_o is the external pressure
P_i is the internal pressure
r_i is the internal radius
r_o is the external radius
r is the variable radius

The canister and plate deflections were also calculated because excessive deflections in the canister could cause the seals to malfunction. The deflection for the plate was calculated at the center because it is the furthest point from the supports and expected to be the greatest. The canister deflection is in the radial direction at the midpoint for the same reason. Both the canister and the caps are assumed to be made of T6 aluminum. The equations used to find the deflections are shown below.

$$\delta_r = \frac{P(r_i + 0.25in)^2}{Et} \quad [8]$$

$$\delta p = \frac{P \bullet r_o^4}{64D} \quad [9]$$

$$D = \frac{E \cdot t_p^3}{12(1-\upsilon^2)} \quad [10]$$

where;

δr is the radial deflection of the canister

P is the external pressure

E is the modulus of Elasticity

t is the thickness of the canister

t_p is the thickness of the plate

υ is poisons ratio

D is the rigidity of the plate

The results of the analysis are shown in *Table 6* below.

Table 6: Shows the result from the thick walled cylinder analysis of the canister.

Radial deflection of the canister	0.0017 inches
Deflection at the center of the plate	0.002586 inches
Maximum tangential stress	-5203 psi
Maximum radial stress	4359 psi

The data for both the FEM analysis and the thick walled cylinder analysis were conclusive. The methods showed that the dimensions of the proposed canister would not implode when exposed to

an external pressure of 600 psi. The resulting safety factor for the canister is 7.68. A complete copy of the analysis and explanation can be found in *appendix D*.

Solenoid Testing: (Hayden Turner, Jud DeCew, Scott Brimlow)

The electro-mechanical torque constant and the resistance torque were the first parameters to be studied. These parameters can be found by varying the mass on the end of the rotary arm. With the use of a power source the required currents and voltages to trigger the solenoid for the changing masses can be recorded. The resistance torque and the torque constant can be obtained by examining the plot of the current versus mass. The setup shown in figure x was used.

The basic procedure for the first experiment was accomplished in the following manner:

1. Measure the electrical resistance of the solenoid.
2. Measure the length of the rotational arm.
3. Vary the mass hanging at the end of the arm from zero to four ounces and record the current when the system moves.
4. Activation voltages can then be solved since the resistance and currents were known
5. The torque constant with respect to current and voltage can be calculated.
6. Solve for the resistance torque.

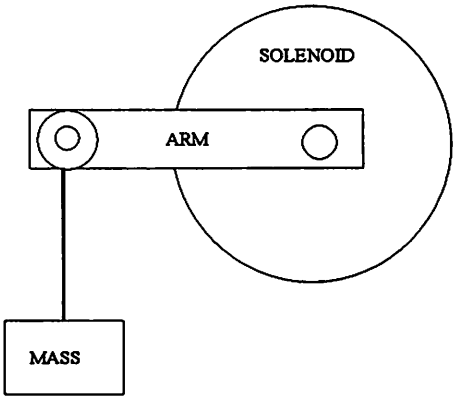

Figure 24: This figure is thesetup used in the first two experiments.

To determine the spring stiffness, k, the spring has to be loaded and unloaded with various weights. A similar setup was used but no power was used and the rotational displacements were recorded. Each mass added created an angular displacement which was recorded using dial calipers and trigonometry.

The procedure for finding the spring stiffness was done by:

1. Load the arm with the various weight used in the previous experiment.

Loading:

2. With the first weight, hold the weight so that no force is applied to the arm, and release gently until the spring force stops it.
3. Record the displacement from a fixed reference point.

Unloading:

4. Turn the solenoid arm to its maximum rotation angle and release the mass gently until the spring force stops it; measure the displacement.

Both:

5. Record all data for each mass.

6. Calculate the angle of rotation for both cases.
7. Find the torque from the weight and the effective torque. The effective torque is the torque caused by the mass of the arm.
8. Find the total torque which is the sum of the torques.
9. Plot the torque versus the angle of rotation for each case. The slope of the line is the spring stiffness k.

The next experiment was used to determine the electrical time constant for the solenoid. The setup for the experiment consisted of a one ohm resistor placed in series with the solenoid and the power supply. The current can be measured across the resistor and the signal stored using an oscilloscope. The time constant can then be determined. For a full description, see appendix D.

The damping and the mass moment of the inertia need to be determined for the mechanical model. Figure x shows the appendix and the step by step instructions are listed below.

1. Solve for J using the values previously determined.
2. Connect a potentiometer to the solenoid and fix both of them to a stationary object.
3. Introduce the solenoid with a 5-volt impulse.
4. Read the potentiometer output using an oscilloscope.
5. Find the break voltages and times.
6. Fit a second order function between the two points and determine the damping ratio.

The solenoid data can be seen in appendix D and the information obtained is shown in *Table 7.*

Table 7: This table shows pertinent information regarding the rotary solenoid.

Mass moment of inertia	3.166×10^{-4} lbf in sec^2
Spring constant	3.089×10^{-3} lbf in/deg
Damping ratio	0.171
Damping constant	4.468×10^{-5} lbf sec in/deg
Torque due to friction	0.066 lbf in
Torque constant with respect to current	1.321 lbf in/amp
Torque constant with respect to voltage	0.212 lbf in/volt
Resistance	10.6 ohm
Inductance	0.029 henry
Tim constant for the system	24 mili sec

Cost Analysis: (Hayden Turner, Jud DeCew)

The prototype cost for the acoustically triggered buoyless lobster trap recovery system was much less than anticipated. Many components of the system were obtained at no cost from old projects or stock material. The cost of the prototype, the cost of a single system built from scratch, and a large scale production unit cost can be seen in *Table 8.*

Table 8: Analysis of costs of producing a lobster trap recovery system.

Component	Prototype Unit	Single Unit	Production Unit
Hydrophone	$ 0.00	$1200.00	$75.00
Container	$136.50	$250.00	$100.00
Solenoid	$110.00	$110.00	$65.00
Winding System	$356.00	$356.00	$15.00
Electrical System	$18.00	$25.00	$10.00
Lobster Trap	$40.00	$40.00	$10.00
Miscellaneous Hardware	$135.30	$255.85	$40.00
Excess / Unused Material	$175.29	$0.00	$0.00
Total	**$971.09**	**$2236.85**	**$315.00**

The table displays the main components of the BLT. For a complete listing of all the prices and components of the system see *appendix F.* The hydro-phone used in the system was taken from an old project and adjusted to fit with the container. The lowered unit cost of the hydrophone is based upon manufacturing costs of gill net pingers.

The container component consists of the pressure vessel, latches, seals and o-rings used in the prototype. In the making of a single unit, the pressure vessel's cost increases because of machining and the aluminum material. When produced on a large scale, it is estimated that the cost will still be considerable due to the machining process. The unit has to be watertight and not rupture under the applied pressures. The rotational solenoid's cost reduces by 40% with manufacturing processes.

The electrical system is composed of individual components which can be supplied at a low cost. The vinyl covered wire lobster trap can be substituted for a wooden one. This allows industry to construct a BLT from existing or older wooden traps.

The hardware includes construction materials such as fasteners and screws, the release bar, the buoy,

line and any tools needed. The buoy used in the prototype was obtained at no cost. A single closed cell foam buoy is needed to go to the required depths (1200 ft). The single unit cost of the buoy is around $150. The excess materials, shown in *Table 8*, were originally needed for the system. The materials were discarded as the system was modified.

The final prototype cost for the prototype of the lobster system was $971.09. The original estimated budget to research this project was $2000. The project finished 51% below the intended cost. This is attributed to the fact that previously used materials were recycled for use in the system and intensive research was performed on all possible items before purchasing to reduce waste spending.

Discussion / Future Considerations (Hayden Turner, Jud DeCew)

The final lobster trap system went through many stages of construction and modification. There are many aspects that need to be ascertained before the BLT is adopted by commercial fishing companies. A lobster boat requires optimal space utilization to carry their equipment. Currently, the lobster trap recovery systems are not stackable due to the protrusion of the hydro-phone. The hydro-phone was acquired from a previous project a few years' prior. The hydrophone is mounted to a metal shaft 8 inches high. The initial design proclaimed that the hydrophone be contained within the trap so it would not interfere with the stacking of the traps.

Another reason why the current trap is not stackable is the key and release arm. The rotational solenoid was to be placed inside the main container, according to the original design. A dynamic shaft seal could not be found as easily as expected. The riposte was to append an oil-filled container to the top of the main pressure vessel to accommodate the solenoid. This container will compensate for the extreme pressure by decreasing the pressure difference across the seal. The added height of the solenoid canister caused the key to penetrate the trap boundary.

Various fluids were researched for the interior of the solenoid container. The desired fluid had to be non-conductive, incompressible, economic, and nontoxic. Silicone Oil would be the ideal choice if it were not so expensive. Vegetable oil was used because of it is environmentally friendly, inexpensive, and easily accessible. Testing on the vegetable oil should be conducted to investigate how the integrity of the oil changes over time. Vegetable oil is a biological product which could promote biological growth after an extended period of time. This could conceivably impair the performance of the solenoid.

Further research of the electronics signal processing, decoding, and modulation needs to be conducted before the system is implemented into the fishing industry. Each owner would possess a transponder with an encrypted code that would be integrated into the pre-existing depth sounding system. This way unexpected release of the buoy can be avoided by other signals or sounds in the water. A sonar pinger would also have to be attached to the gear for location purposed in case of equipment failure. Grappling for the lost gear could be done through the use of the locating signal. Testing needs to be done to determine the life of the batteries used to power the system. The exact current draw by the electronics is not known, and needs to be evaluated so the users know how often to change the batteries. The average deep sea ocean temperature is roughly 4 degrees Celsius, which can have adverse effects on battery life.

The analysis of the rising buoy has to be evaluated experimentally to verify the mathematical models. Deep water testing of the system is the only way to determine the actual rise time for the buoy. Testing should be done to verify that the system will behave as predicted by the various models. The frictional forces of the spool were ignored and this could cause the system to react in an unpredictable manner.

The winding mechanism can easily be modified so that a pneumatic drill could be used to rewind the line. Another alternative would be to make the spool detachable so that winding of the line could be done on deck. This could save time during the retrieval. Line testing may prove the spool to be a useless endeavor. If a separate line container or coiling of the line would work as well then the spool would become obsolete.

For the prototype system, hard plastic trawl buoys with eight pounds of buoyancy were used to bring up the line. These buoys will implode at a depth of 1,200 ft but would be acceptable for the prototype. A closed cell foam buoy would need to be used for a depth of 1,200 feet.

A trawl resistant trap was the original intention for the recovery system but, the system was modified to mate with a regular lobster trap for convenience. The recovered components could be placed into another trap if the system were destroyed by a fishing vessel. This reduced the cost of the system greatly.

Appendix A

Buoy Analysis

Appendix A:

Estimation of forces on the buoy using a time step approach (Hayden Turner)

FBD

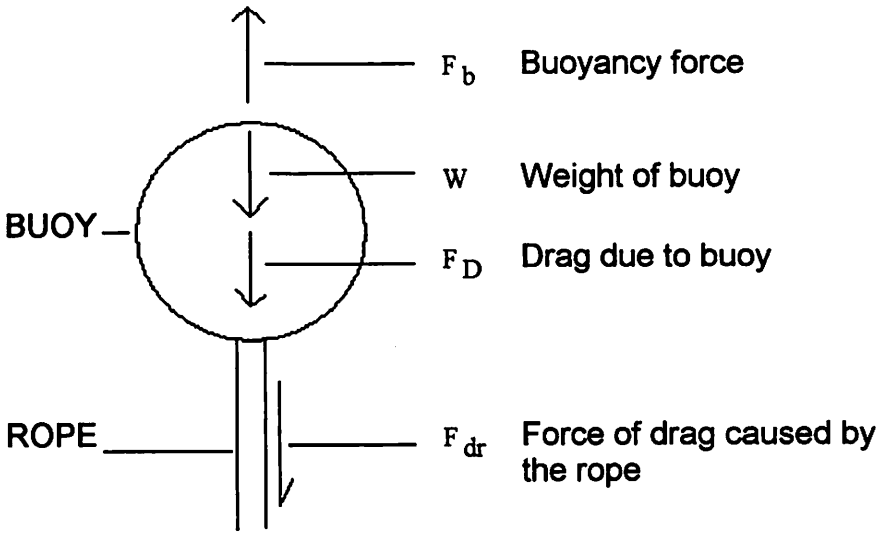

Resulting equations of motion:

$$F_b - W - F_D - F_{dr} = M \cdot a$$

$$F_b = \rho_w \cdot g \cdot V \qquad W := 1 \cdot lbf \qquad F_D = 3 \cdot \pi \cdot \mu \cdot V \cdot l$$

$$F_{dr} = \frac{1}{2} \cdot C_D \cdot A \cdot \rho_w \cdot U^2 \qquad M := \frac{W}{g} \qquad M = 0.454 \cdot kg$$

Assumptions:

-kinematic viscosity is constant

-density of the seawater is constant

-the buoy is rigid

-the rope is buoyant

$L := 1400 \cdot ft$ Maximum length of rope

$\rho_w := 1027.7 \cdot \frac{kg}{m^3}$ Average density of sea water

$\mu := 1.08 \cdot 10^{-3} \cdot \frac{kg}{m \cdot sec}$ Average dynamic viscosity

$\nu := 1.6094 \cdot 10^{-3} \cdot \frac{m^2}{sec}$ Average kinematic viscosity

$ra := 4 \cdot in$ $ra = 0.102 \cdot m$ Radius of the buoy

$V := \frac{4}{3} \cdot ra^3 \cdot \pi$ $V = 4.393 \cdot 10^{-3} \cdot m^3$ $V = 268.083 \cdot in^3$ Volume of the buoy

$r := \frac{6.35 \cdot 10^{-3} \cdot m}{2}$ $r = 0.125 \cdot in$ Radius of the rope

$W = 4.448 \cdot newton$ Weight of the buoy

Begin the simulation by finding the terminal velocity assuming the worst case conditions.

$ORIGIN := 1$

q_1 is the position in m $q'(t,q)$ is the accelleration m/s^2

q_2 is the velocity in m/s

$Re_L(q) := \frac{q_2 \cdot \frac{m}{sec} \cdot q_1 \cdot m}{\nu}$ Reynolds Number

$$C_D(q) := \begin{cases} \left(\frac{0.445}{\log(Re_L(q))^{2.58}} - \frac{1610}{Re_L(q)} \right) & \text{if } 1 \cdot 10^7 \le Re_L(q) \le 1 \cdot 10^9 \\ \left(\frac{0.074}{Re_L(q)^{\frac{1}{5}}} - \frac{1740}{Re_L(q)} \right) & \text{if } 5 \cdot 10^5 < Re_L(q) < 1 \cdot 10^7 \\ \frac{0.455}{\log(Re_L(q))^{2.58}} & \text{if } 2300 \le Re_L(q) \le 5 \cdot 10^5 \\ \frac{64}{Re_L(q)} & \text{otherwise} \end{cases}$$ Drag Coefficient

$wc := \begin{pmatrix} \frac{L}{m} \\ 2.4 \end{pmatrix}$ worst case conditions

$vel := 5$

Given

$$\left[\frac{1}{M}\cdot\left[\rho_w\cdot g\cdot V - W - 3\cdot\pi\cdot\mu\cdot 2\cdot ra\cdot vel\cdot\frac{m}{sec} - \frac{1}{2}\cdot C_D(wc)\cdot\rho_w\cdot vel^2\cdot 2\cdot\pi\cdot r\cdot wc_1\cdot m\cdot\left(\frac{m}{sec}\right)^2\right]\right]=0$$

$v_t := \text{Find}(vel)$

$v_{term} := v_t\cdot\frac{m}{sec}$

$v_{term} = 1.957\cdot\frac{m}{sec}$ $v_{term} = 4.378\cdot mph$ Estimated terminal velocity

$time := \frac{1400\cdot ft}{v_{term}}$ $time = 3.634\cdot min$ $time = 218.02\cdot sec$ Estimated time required by the buoy to reach the surface.

Since the terminal velocity is not constant, due to an increase in the line drag, the following simulation will use the preceeded value of q2 (velocity) if it should go negative.

$$F_d(q) := \frac{1}{2}\cdot C_D(q)\cdot\frac{\rho_w}{\left(\frac{kg}{m^3}\right)}\cdot(q_2)^2\cdot 2\cdot\pi\cdot\frac{r}{m}\cdot q_1$$ Force of drag due to the rope

$acc := 9.8$ Acceleration due to gravity

$ma := 4.444$ Weight of the buoy in newtons

$$q'(t,q) := \begin{cases} \left[\left[\frac{1}{ma}\cdot\left[\frac{\rho_w}{\left(\frac{kg}{m^3}\right)}\cdot acc\cdot\frac{V}{m^3} - 38\cdot\pi\cdot\frac{\mu}{\frac{kg}{m\cdot sec}}\cdot 2\cdot\frac{ra}{m}\cdot q_2 - F_d(q)\right]\right]\right] & \text{if } q_2 > 0 \\ \left[\left[\frac{1}{ma}\cdot\left[\frac{\rho_w}{\left(\frac{kg}{m^3}\right)}\cdot acc\cdot\frac{V}{m^3} - 38\cdot\pi\cdot\frac{\mu}{\frac{kg}{m\cdot sec}}\cdot 2\cdot\frac{ra}{m}\cdot q_2 - F_d(q)\right]\right]\right] & \text{if } q_2 \le 0 \end{cases}$$

$q^{\langle 1 \rangle} := \begin{pmatrix} 1 \\ .000001 \end{pmatrix}$ Initial conditions

$\Delta t := 0.1$ Time step in seconds $t_f := 250$ Final time in seconds

$N := \text{ceil}\left(\frac{t_f}{\Delta t}\right)$ $N = 2.5 \cdot 10^3$ Total number of iterations

$n := 1 .. N$ $t_n := n \cdot \Delta t$ Initializes the time step matrix

$q^{\langle n+1 \rangle} := q^{\langle n \rangle} + q'\left(t_n, q^{\langle n \rangle}\right) \cdot \Delta t$ Euler integration

$\text{Surface} := 426$ Distance from the ocean floor to the surface

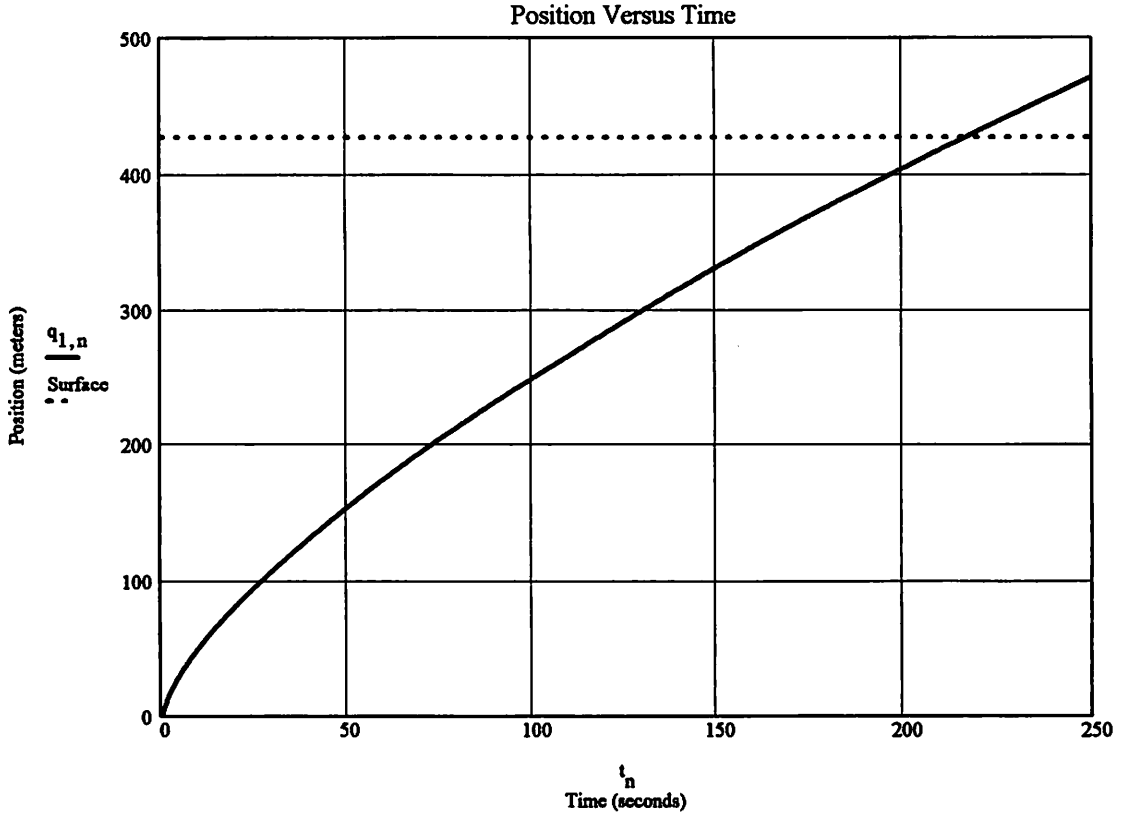

Figure A1: This figure shows how the retrieval buoy will rise to the surface over time. By looking at the graph at the point where the Surface line and the position curve intersect we can see that the time required to come to the surface is approximately 220 seconds which is very close to the previous estimation of 218 seconds.

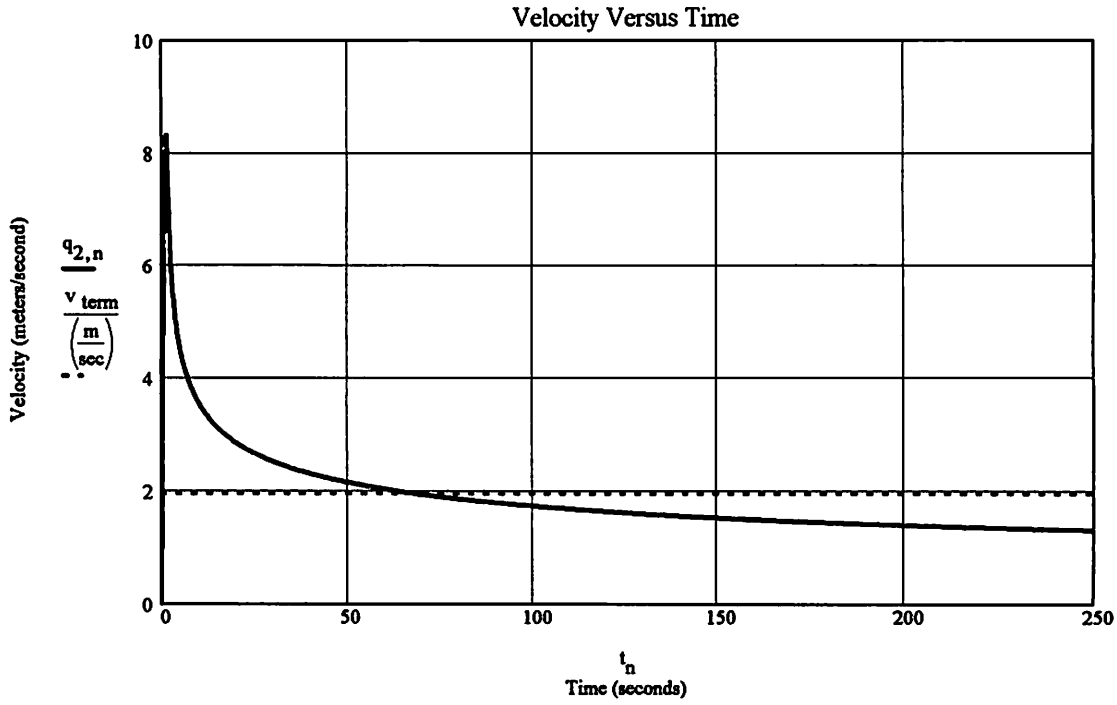

Figure A2: This plot shows the velocity of the the buoy as a function of time. The velocity has a spike in the first ten second but slows down considerably as more and more line enters the water column. The dotted line indicates the previous estimation for the terminal velocity of the buoy.

Buoy analysis using a depth step approach (Jud DeCew)

$\nu := (1.6094 \cdot 10^{-6}) \cdot \frac{m^2}{sec}$ kinematic viscousity is constant

$\mu := 1.08 \cdot 10^{-3} \cdot \frac{kg}{m \cdot sec}$ dynamic viscousity is constant

$\rho := 1025.7 \cdot \frac{kg}{m^3}$ density is contstant

$r_{buoy} := \frac{.305}{2} \cdot m$ radius of buoy is constant

$vol := \frac{4}{3} \cdot r_{buoy}^3 \cdot \pi$ Volume of the buoy

$r_{rope} := 6.35 \cdot 10^{-3} \cdot m$ radius of the rope

$m_{buoy} := 4.448 \cdot kg$ Weight of buoy

$g = 9.807 \cdot m \cdot sec^{-2}$ Acceleration due to gravity

According to the free body diagram, the forces are shown below:

$\sum F = 0$

$F = F_{buoyant} + W_{buoy} + D_{buoy} + D_{rope} = 0$

Newton's second law states:

$F = m \cdot a$

Therefore

$$a = \frac{F_{buoyant} + W_{buoy} + D_{buoy} + D_{rope}}{m}$$

$F_{buoyant} := \rho \cdot g \cdot vol$ Buoyant Force

$W_{buoy} := m_{buoy} \cdot g$ Weight of the Buoy

$D_{buoy}(V) = .5 \cdot \rho \cdot V^2 \cdot S_{buoy} \cdot C_{d1}$ Drag of the Buoy

$S_s(L) := \pi \cdot 2 \cdot r_{rope} \cdot L$ Surface Area of the Rope

$C_{d2} := .05$ Coefficent of drag for the rope

$D_{rope}(V, L) := .5 \cdot \rho \cdot V^2 \cdot S_s(L) \cdot C_{d2}$ Drag of the Rope

$$R=\frac{d_{rope}\cdot V\cdot \rho}{\mu}$$

Reynolds Number - Checks the flow to see if it is laminar or turbulent

$$DF=F_{buoyant}-W_{buoy}$$

These forces are constant

$$TotalD=DF+D_{buoy}+D_{rope}$$

Total Drag force acting upon the system

$$V=\frac{-b+\sqrt{b^2-4\cdot a\cdot c}}{2\cdot a}$$

Velocity of the bouy

where

$$a=.5\cdot\rho\cdot S_{buoy}\cdot C_{d1}+.5\cdot\rho\cdot\left(\pi\cdot 2\cdot r_{rope}\cdot L\right)\cdot C_{d2}$$

$$b=0$$

$$c=F_{buoyant}-W_{buoy}$$

$$V=\frac{0+\sqrt{0^2-4\cdot\left[.5\cdot\rho\cdot S_{buoy}\cdot C_{d1}+.5\cdot\rho\cdot\left(\pi\cdot 2\cdot r_{rope}\cdot L\right)\cdot C_{d2}\right]\cdot\left(F_{buoyant}-W_{buoy}\right)}}{2\cdot\left[.5\cdot\rho\cdot S_{buoy}\cdot C_{d1}+.5\cdot\rho\cdot\left(\pi\cdot 2\cdot r_{rope}\cdot L\right)\cdot C_{d2}\right]}$$

$$AveV=\frac{V_1+V_2}{2}$$

Average velocity of the buoy between two distances

$$Dtime=\frac{distance_2-distance_1}{time}$$

Change in time of the buoy from one measuring point to the next

Appendix A:

Estimation of foces using a depth step approach: (Jud DeCew)

distance	Renaulds	DF	Drag rope	Drag buoy	Total D	V elocity	Ave Vel	Dtime	time
m	---	kg-m/s^2	kg-m/s^2	kg-m/s^2	kg-m/s^2	m/s	m/s	sec	sec
0	0.00E+00	0	0.000	0.00	0	0	0	0.00	0.00
2.5	4.69E+08	-102.04	2.558	14.99	17.549	2.4113	1.2057	2.07	2.07
5	4.38E+08	-102.04	5.116	14.99	20.107	2.2527	2.3320	1.07	3.15
7.5	4.13E+08	-102.04	7.675	14.99	22.665	2.1218	2.1873	1.14	4.29
10	3.91E+08	-102.04	10.233	14.99	25.224	2.0113	2.0666	1.21	5.50
12.5	3.73E+08	-102.04	12.791	14.99	27.782	1.9165	1.9639	1.27	6.77
15	3.57E+08	-102.04	15.349	14.99	30.340	1.8339	1.8752	1.33	8.10
17.5	3.42E+08	-102.04	17.908	14.99	32.898	1.7612	1.7975	1.39	9.50
20	3.30E+08	-102.04	20.466	14.99	35.457	1.6964	1.7288	1.45	10.94
22.5	3.19E+08	-102.04	23.024	14.99	38.015	1.6384	1.6674	1.50	12.44
25	3.08E+08	-102.04	25.582	14.99	40.573	1.5859	1.6121	1.55	13.99
27.5	2.99E+08	-102.04	28.140	14.99	43.131	1.5381	1.5620	1.60	15.59
30	2.91E+08	-102.04	30.699	14.99	45.689	1.4944	1.5163	1.65	17.24
32.5	2.83E+08	-102.04	33.257	14.99	48.248	1.4543	1.4744	1.70	18.94
35	2.76E+08	-102.04	35.815	14.99	50.806	1.4172	1.4357	1.74	20.68
37.5	2.69E+08	-102.04	38.373	14.99	53.364	1.3828	1.4000	1.79	22.46
40	2.63E+08	-102.04	40.932	14.99	55.922	1.3508	1.3668	1.83	24.29
42.5	2.57E+08	-102.04	43.490	14.99	58.481	1.3209	1.3359	1.87	26.16
45	2.51E+08	-102.04	46.048	14.99	61.039	1.2930	1.3069	1.91	28.08
47.5	2.46E+08	-102.04	48.606	14.99	63.597	1.2667	1.2798	1.95	30.03
50	2.41E+08	-102.04	51.164	14.99	66.155	1.2419	1.2543	1.99	32.02
52.5	2.37E+08	-102.04	53.723	14.99	68.713	1.2186	1.2303	2.03	34.06
55	2.33E+08	-102.04	56.281	14.99	71.272	1.1965	1.2076	2.07	36.13
57.5	2.29E+08	-102.04	58.839	14.99	73.830	1.1756	1.1861	2.11	38.23
60	2.25E+08	-102.04	61.397	14.99	76.388	1.1558	1.1657	2.14	40.38
62.5	2.21E+08	-102.04	63.956	14.99	78.946	1.1369	1.1463	2.18	42.56
65	2.18E+08	-102.04	66.514	14.99	81.505	1.1189	1.1279	2.22	44.78
67.5	2.14E+08	-102.04	69.072	14.99	84.063	1.1018	1.1103	2.25	47.03
70	2.11E+08	-102.04	71.630	14.99	86.621	1.0854	1.0936	2.29	49.31
72.5	2.08E+08	-102.04	74.188	14.99	89.179	1.0697	1.0775	2.32	51.63
75	2.05E+08	-102.04	76.747	14.99	91.737	1.0547	1.0622	2.35	53.99
77.5	2.02E+08	-102.04	79.305	14.99	94.296	1.0403	1.0475	2.39	56.37
80	2.00E+08	-102.04	81.863	14.99	96.854	1.0264	1.0333	2.42	58.79
82.5	1.97E+08	-102.04	84.421	14.99	99.412	1.0131	1.0198	2.45	61.24
85	1.94E+08	-102.04	86.980	14.99	101.970	1.0003	1.0067	2.48	63.73
87.5	1.92E+08	-102.04	89.538	14.99	104.529	0.9880	0.9942	2.51	66.24
90	1.90E+08	-102.04	92.096	14.99	107.087	0.9762	0.9821	2.55	68.79
92.5	1.88E+08	-102.04	94.654	14.99	109.645	0.9647	0.9704	2.58	71.36
95	1.85E+08	-102.04	97.212	14.99	112.203	0.9536	0.9592	2.61	73.97
97.5	1.83E+08	-102.04	99.771	14.99	114.761	0.9429	0.9483	2.64	76.61
100	1.81E+08	-102.04	102.329	14.99	117.320	0.9326	0.9378	2.67	79.27
102.5	1.79E+08	-102.04	104.887	14.99	119.878	0.9226	0.9276	2.70	81.97
105	1.77E+08	-102.04	107.445	14.99	122.436	0.9129	0.9178	2.72	84.69
107.5	1.76E+08	-102.04	110.004	14.99	124.994	0.9035	0.9082	2.75	87.44
110	1.74E+08	-102.04	112.562	14.99	127.553	0.8944	0.8990	2.78	90.23
112.5	1.72E+08	-102.04	115.120	14.99	130.111	0.8856	0.8900	2.81	93.03
115	1.71E+08	-102.04	117.678	14.99	132.669	0.8770	0.8813	2.84	95.87
117.5	1.69E+08	-102.04	120.236	14.99	135.227	0.8687	0.8728	2.86	98.74
120	1.67E+08	-102.04	122.795	14.99	137.785	0.8606	0.8646	2.89	101.63
122.5	1.66E+08	-102.04	125.353	14.99	140.344	0.8527	0.8566	2.92	104.55
125	1.64E+08	-102.04	127.911	14.99	142.902	0.8450	0.8489	2.95	107.49
127.5	1.63E+08	-102.04	130.469	14.99	145.460	0.8376	0.8413	2.97	110.46

distance	Renaulds	DF	Drag rope	Drag buoy	Total D	V elocity	Ave Vel	Dtime	time
m	---	kg-m/s^2	kg-m/s^2	kg-m/s^2	kg-m/s^2	m/s	m/s	sec	sec
130	1.61E+08	-102.04	133.028	14.99	148.018	0.8303	0.8339	3.00	113.46
132.5	1.60E+08	-102.04	135.586	14.99	150.577	0.8232	0.8267	3.02	116.48
135	1.59E+08	-102.04	138.144	14.99	153.135	0.8163	0.8197	3.05	119.53
137.5	1.57E+08	-102.04	140.702	14.99	155.693	0.8096	0.8129	3.08	122.61
140	1.56E+08	-102.04	143.260	14.99	158.251	0.8030	0.8063	3.10	125.71
142.5	1.55E+08	-102.04	145.819	14.99	160.809	0.7966	0.7998	3.13	128.84
145	1.54E+08	-102.04	148.377	14.99	163.368	0.7903	0.7934	3.15	131.99
147.5	1.52E+08	-102.04	150.935	14.99	165.926	0.7842	0.7873	3.18	135.16
150	1.51E+08	-102.04	153.493	14.99	168.484	0.7782	0.7812	3.20	138.36
152.5	1.50E+08	-102.04	156.052	14.99	171.042	0.7724	0.7753	3.22	141.59
155	1.49E+08	-102.04	158.610	14.99	173.601	0.7667	0.7695	3.25	144.84
157.5	1.48E+08	-102.04	161.168	14.99	176.159	0.7611	0.7639	3.27	148.11
160	1.47E+08	-102.04	163.726	14.99	178.717	0.7556	0.7584	3.30	151.40
162.5	1.46E+08	-102.04	166.284	14.99	181.275	0.7503	0.7529	3.32	154.73
165	1.45E+08	-102.04	168.843	14.99	183.833	0.7450	0.7476	3.34	158.07
167.5	1.44E+08	-102.04	171.401	14.99	186.392	0.7399	0.7425	3.37	161.44
170	1.43E+08	-102.04	173.959	14.99	188.950	0.7349	0.7374	3.39	164.83
172.5	1.42E+08	-102.04	176.517	14.99	191.508	0.7299	0.7324	3.41	168.24
175	1.41E+08	-102.04	179.076	14.99	194.066	0.7251	0.7275	3.44	171.68
177.5	1.40E+08	-102.04	181.634	14.99	196.625	0.7204	0.7228	3.46	175.14
180	1.39E+08	-102.04	184.192	14.99	199.183	0.7157	0.7181	3.48	178.62
182.5	1.38E+08	-102.04	186.750	14.99	201.741	0.7112	0.7135	3.50	182.12
185	1.37E+08	-102.04	189.308	14.99	204.299	0.7067	0.7090	3.53	185.65
187.5	1.37E+08	-102.04	191.867	14.99	206.857	0.7023	0.7045	3.55	189.20
190	1.36E+08	-102.04	194.425	14.99	209.416	0.6980	0.7002	3.57	192.77
192.5	1.35E+08	-102.04	196.983	14.99	211.974	0.6938	0.6959	3.59	196.36
195	1.34E+08	-102.04	199.541	14.99	214.532	0.6897	0.6917	3.61	199.97
197.5	1.33E+08	-102.04	202.100	14.99	217.090	0.6856	0.6876	3.64	203.61
200	1.33E+08	-102.04	204.658	14.99	219.649	0.6816	0.6836	3.66	207.27
202.5	1.32E+08	-102.04	207.216	14.99	222.207	0.6777	0.6796	3.68	210.94
205	1.31E+08	-102.04	209.774	14.99	224.765	0.6738	0.6757	3.70	214.64
207.5	1.30E+08	-102.04	212.332	14.99	227.323	0.6700	0.6719	3.72	218.36
210	1.30E+08	-102.04	214.891	14.99	229.881	0.6662	0.6681	3.74	222.11
212.5	1.29E+08	-102.04	217.449	14.99	232.440	0.6626	0.6644	3.76	225.87
215	1.28E+08	-102.04	220.007	14.99	234.998	0.6590	0.6608	3.78	229.65
217.5	1.27E+08	-102.04	222.565	14.99	237.556	0.6554	0.6572	3.80	233.46
220	1.27E+08	-102.04	225.124	14.99	240.114	0.6519	0.6536	3.82	237.28
222.5	1.26E+08	-102.04	227.682	14.99	242.673	0.6484	0.6502	3.85	241.13
225	1.25E+08	-102.04	230.240	14.99	245.231	0.6451	0.6468	3.87	244.99
227.5	1.25E+08	-102.04	232.798	14.99	247.789	0.6417	0.6434	3.89	248.88
230	1.24E+08	-102.04	235.356	14.99	250.347	0.6384	0.6401	3.91	252.78
232.5	1.23E+08	-102.04	237.915	14.99	252.905	0.6352	0.6368	3.93	256.71
235	1.23E+08	-102.04	240.473	14.99	255.464	0.6320	0.6336	3.95	260.65
237.5	1.22E+08	-102.04	243.031	14.99	258.022	0.6289	0.6304	3.97	264.62
240	1.22E+08	-102.04	245.589	14.99	260.580	0.6258	0.6273	3.99	268.61
242.5	1.21E+08	-102.04	248.148	14.99	263.138	0.6227	0.6242	4.00	272.61
245	1.20E+08	-102.04	250.706	14.99	265.697	0.6197	0.6212	4.02	276.63
247.5	1.20E+08	-102.04	253.264	14.99	268.255	0.6168	0.6182	4.04	280.68
250	1.19E+08	-102.04	255.822	14.99	270.813	0.6138	0.6153	4.06	284.74
252.5	1.19E+08	-102.04	258.380	14.99	273.371	0.6110	0.6124	4.08	288.82
255	1.18E+08	-102.04	260.939	14.99	275.929	0.6081	0.6095	4.10	292.93
257.5	1.18E+08	-102.04	263.497	14.99	278.488	0.6053	0.6067	4.12	297.05
260	1.17E+08	-102.04	266.055	14.99	281.046	0.6026	0.6039	4.14	301.19
262.5	1.17E+08	-102.04	268.613	14.99	283.604	0.5998	0.6012	4.16	305.34

distance	Renaulds	DF	Drag rope	Drag buoy	Total D	V elocity	Ave Vel	Dtime	time
m	---	kg-m/s^2	kg-m/s^2	kg-m/s^2	kg-m/s^2	m/s	m/s	sec	sec
265	1.16E+08	-102.04	271.172	14.99	286.162	0.5971	0.5985	4.18	309.52
267.5	1.16E+08	-102.04	273.730	14.99	288.721	0.5945	0.5958	4.20	313.72
270	1.15E+08	-102.04	276.288	14.99	291.279	0.5919	0.5932	4.21	317.93
272.5	1.15E+08	-102.04	278.846	14.99	293.837	0.5893	0.5906	4.23	322.16
275	1.14E+08	-102.04	281.404	14.99	296.395	0.5867	0.5880	4.25	326.42
277.5	1.14E+08	-102.04	283.963	14.99	298.953	0.5842	0.5855	4.27	330.69
280	1.13E+08	-102.04	286.521	14.99	301.512	0.5817	0.5830	4.29	334.97
282.5	1.13E+08	-102.04	289.079	14.99	304.070	0.5793	0.5805	4.31	339.28
285	1.12E+08	-102.04	291.637	14.99	306.628	0.5769	0.5781	4.32	343.61
287.5	1.12E+08	-102.04	294.196	14.99	309.186	0.5745	0.5757	4.34	347.95
290	1.11E+08	-102.04	296.754	14.99	311.745	0.5721	0.5733	4.36	352.31
292.5	1.11E+08	-102.04	299.312	14.99	314.303	0.5698	0.5710	4.38	356.69
295	1.10E+08	-102.04	301.870	14.99	316.861	0.5675	0.5686	4.40	361.08
297.5	1.10E+08	-102.04	304.428	14.99	319.419	0.5652	0.5663	4.41	365.50
300	1.09E+08	-102.04	306.987	14.99	321.977	0.5630	0.5641	4.43	369.93
302.5	1.09E+08	-102.04	309.545	14.99	324.536	0.5607	0.5618	4.45	374.38
305	1.09E+08	-102.04	312.103	14.99	327.094	0.5585	0.5596	4.47	378.85
307.5	1.08E+08	-102.04	314.661	14.99	329.652	0.5564	0.5574	4.48	383.33
310	1.08E+08	-102.04	317.220	14.99	332.210	0.5542	0.5553	4.50	387.83
312.5	1.07E+08	-102.04	319.778	14.99	334.769	0.5521	0.5532	4.52	392.35
315	1.07E+08	-102.04	322.336	14.99	337.327	0.5500	0.5510	4.54	396.89
317.5	1.07E+08	-102.04	324.894	14.99	339.885	0.5479	0.5490	4.55	401.44
320	1.06E+08	-102.04	327.452	14.99	342.443	0.5459	0.5469	4.57	406.02
322.5	1.06E+08	-102.04	330.011	14.99	345.001	0.5438	0.5449	4.59	410.60
325	1.05E+08	-102.04	332.569	14.99	347.560	0.5418	0.5428	4.61	415.21
327.5	1.05E+08	-102.04	335.127	14.99	350.118	0.5399	0.5408	4.62	419.83
330	1.05E+08	-102.04	337.685	14.99	352.676	0.5379	0.5389	4.64	424.47
332.5	1.04E+08	-102.04	340.244	14.99	355.234	0.5360	0.5369	4.66	429.13
335	1.04E+08	-102.04	342.802	14.99	357.793	0.5340	0.5350	4.67	433.80
337.5	1.03E+08	-102.04	345.360	14.99	360.351	0.5321	0.5331	4.69	438.49
340	1.03E+08	-102.04	347.918	14.99	362.909	0.5303	0.5312	4.71	443.20
342.5	1.03E+08	-102.04	350.476	14.99	365.467	0.5284	0.5293	4.72	447.92
345	1.02E+08	-102.04	353.035	14.99	368.025	0.5266	0.5275	4.74	452.66
347.5	1.02E+08	-102.04	355.593	14.99	370.584	0.5247	0.5256	4.76	457.42
350	1.02E+08	-102.04	358.151	14.99	373.142	0.5229	0.5238	4.77	462.19
352.5	1.01E+08	-102.04	360.709	14.99	375.700	0.5212	0.5220	4.79	466.98
355	1.01E+08	-102.04	363.268	14.99	378.258	0.5194	0.5203	4.81	471.78
357.5	1.01E+08	-102.04	365.826	14.99	380.817	0.5176	0.5185	4.82	476.60
360	1.00E+08	-102.04	368.384	14.99	383.375	0.5159	0.5168	4.84	481.44
362.5	1.00E+08	-102.04	370.942	14.99	385.933	0.5142	0.5151	4.85	486.29
365	9.96E+07	-102.04	373.500	14.99	388.491	0.5125	0.5133	4.87	491.16
367.5	9.93E+07	-102.04	376.059	14.99	391.049	0.5108	0.5117	4.89	496.05
370	9.90E+07	-102.04	378.617	14.99	393.608	0.5092	0.5100	4.90	500.95
372.5	9.87E+07	-102.04	381.175	14.99	396.166	0.5075	0.5083	4.92	505.87
375	9.84E+07	-102.04	383.733	14.99	398.724	0.5059	0.5067	4.93	510.80
377.5	9.80E+07	-102.04	386.292	14.99	401.282	0.5043	0.5051	4.95	515.75
380	9.77E+07	-102.04	388.850	14.99	403.841	0.5027	0.5035	4.97	520.72
382.5	9.74E+07	-102.04	391.408	14.99	406.399	0.5011	0.5019	4.98	525.70
385	9.71E+07	-102.04	393.966	14.99	408.957	0.4995	0.5003	5.00	530.70
387.5	9.68E+07	-102.04	396.524	14.99	411.515	0.4980	0.4987	5.01	535.71
390	9.65E+07	-102.04	399.083	14.99	414.073	0.4964	0.4972	5.03	540.74
392.5	9.62E+07	-102.04	401.641	14.99	416.632	0.4949	0.4957	5.04	545.78
395	9.59E+07	-102.04	404.199	14.99	419.190	0.4934	0.4941	5.06	550.84
397.5	9.56E+07	-102.04	406.757	14.99	421.748	0.4919	0.4926	5.07	555.92

distance	Renaulds	DF	Drag rope	Drag buoy	Total D	V elocity	Ave Vel	Dtime	time
m	---	kg-m/s^2	kg-m/s^2	kg-m/s^2	kg-m/s^2	m/s	m/s	sec	sec
400	9.53E+07	-102.04	409.316	14.99	424.306	0.4904	0.4911	5.09	561.01
402.5	9.51E+07	-102.04	411.874	14.99	426.865	0.4889	0.4897	5.11	566.11
405	9.48E+07	-102.04	414.432	14.99	429.423	0.4875	0.4882	5.12	571.23
407.5	9.45E+07	-102.04	416.990	14.99	431.981	0.4860	0.4867	5.14	576.37
410	9.42E+07	-102.04	419.548	14.99	434.539	0.4846	0.4853	5.15	581.52
412.5	9.39E+07	-102.04	422.107	14.99	437.097	0.4832	0.4839	5.17	586.69
415	9.37E+07	-102.04	424.665	14.99	439.656	0.4818	0.4825	5.18	591.87
417.5	9.34E+07	-102.04	427.223	14.99	442.214	0.4804	0.4811	5.20	597.07
420	9.31E+07	-102.04	429.781	14.99	444.772	0.4790	0.4797	5.21	602.28
422.5	9.29E+07	-102.04	432.340	14.99	447.330	0.4776	0.4783	5.23	607.51
425	9.26E+07	-102.04	434.898	14.99	449.889	0.4762	0.4769	5.24	612.75
427.5	9.23E+07	-102.04	437.456	14.99	452.447	0.4749	0.4756	5.26	618.00

Constants

μ	1.61E-06	m^3/kg
ρ	1025.9	kg/m^3
rope dia.	6.35E-03	m
buoy rad.	0.1525	m
Cd (rope)	0.05	
Cd (buoy)	0.1	

Time to reach surface
10.3 min

Appendix B

Key Forces

Appendix B:

The initial forces on the key or release mechanism (Hayden Turner)

$L := 1400 \cdot ft$ Maximum length of rope

$ORIGIN := 1$

$\rho_w := 1027.7 \cdot \frac{kg}{m^3}$ Average density of sea water

$\mu := 1.08 \cdot 10^{-3} \cdot \frac{kg}{m \cdot sec}$ Average dynamic viscosity

$\nu := 1.6094 \cdot 10^{-3} \cdot \frac{m^2}{sec}$ Average kinematic viscosity

$ra := 4 \cdot in \qquad ra = 0.102 \cdot m$ Radius of the buoy

$V := \frac{4}{3} \cdot ra^3 \cdot \pi \qquad V = 4.393 \cdot 10^{-3} \cdot m^3 \qquad V = 268.083 \cdot in^3$ Volume of the buoy

$r := \frac{6.35 \cdot 10^{-3} \cdot m}{2} \qquad r = 0.125 \cdot in$ Radius of the rope

$W := 4.448 \cdot newton$ Weight of the buoy

$Re_L(q) := \frac{q_2 \cdot \frac{m}{sec} \cdot q_1 \cdot m}{\nu}$ Reynolds Number

$$C_D(q) := \begin{cases} \left(\frac{0.445}{\log(Re_L(q))^{2.58}} - \frac{1610}{Re_L(q)} \right) & \text{if } 1 \cdot 10^7 \le Re_L(q) \le 1 \cdot 10^9 \\ \left(\frac{0.074}{Re_L(q)^{\frac{1}{5}}} - \frac{1740}{Re_L(q)} \right) & \text{if } 5 \cdot 10^5 < Re_L(q) < 1 \cdot 10^7 \\ \frac{0.455}{\log(Re_L(q))^{2.58}} & \text{if } 2300 \le Re_L(q) \le 5 \cdot 10^5 \\ \frac{64}{Re_L(q)} & \text{otherwise} \end{cases}$$ Drag Coefficient

$wc := \left(\frac{L}{m} \right)_{2.4}$ worst case conditions $\qquad M := \frac{W}{g}$ Mass of buoy

$vel := 0$ Initial velocity

$$\left[\frac{1}{M}\cdot\left[\rho_w\cdot g\cdot V - W - 3\cdot\pi\cdot\mu\cdot 2\cdot ra\cdot vel\cdot\frac{m}{sec} - \frac{1}{2}\cdot C_D(wc)\cdot\rho_w\cdot vel^2\cdot 2\cdot\pi\cdot r\cdot wc_1\cdot m\cdot\left(\frac{m}{sec}\right)^2\right]\right]=0$$

$$F_{in} := \left[\left[\rho_w\cdot g\cdot V - W - 3\cdot\pi\cdot\mu\cdot 2\cdot ra\cdot vel\cdot\frac{m}{sec} - \frac{1}{2}\cdot C_D(wc)\cdot\rho_w\cdot vel^2\cdot 2\cdot\pi\cdot r\cdot wc_1\cdot m\cdot\left(\frac{m}{sec}\right)^2\right]\right]$$

$F_{in} = 39.827\cdot newton$ Initial force on the key and bar

$F_{in} = 8.953\cdot lbf$

There will be two sides to the key so we can divide the force by 2. Then we will assume that the force acts at one point on the side of the key so that we can find the torque needed by the solenoid.

$F := \frac{F_{in}}{2}$ Force is taken up by each side $F = 4.477\cdot lbf$

$\mu_{key} := 1\cdot 10^{-3}$ Approximate value for the coefficient of friction for delrin which is a water lubricated material that resists biological growth.

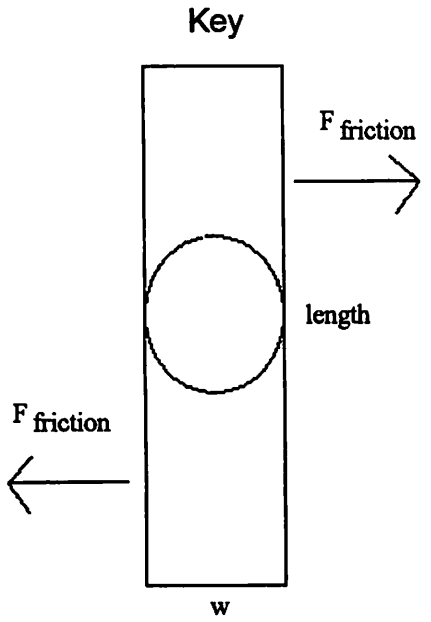

$F_{friction} := \mu_{key}\cdot F$

$F_{friction} = 0.02\cdot newton$

$F_{friction} = 4.477\cdot 10^{-3}\cdot lbf$

Sum the moments about the center in order to find the torque needed by the rotary solenoid.

$T - 2\cdot F_{friction}\cdot\frac{L_{key}}{2} = 0$ $T = 2\cdot F_{friction}\cdot\frac{L_{key}}{4}$ Solve for torque

$L_{key} := \left(1 + \frac{1}{2}\right) \cdot in$ $L_{key} = 0.038 \cdot m$ $L_{key} = 1.5 \cdot in$ Length of the key

$T := F_{friction} \cdot \frac{L_{key}}{2} + F_{friction} \cdot \frac{L_{key}}{2}$ Assume the friction acts at the furthest point from the center to be safe.

$T = 7.587 \cdot 10^{-4} \cdot m \cdot newton$

$T = 6.715 \cdot 10^{-3} \cdot lbf \cdot in$ Torque needed to overcome friction

$T_{safe} := 20 \cdot T$

$T_{safe} = 0.134 \cdot lbf \cdot in$ A safety factor of 20 was used because of extremely high frictional forces expected in the water seals which need to withstand a pressure of 600 psi.

<u>Decrease the torque needed by reducing the moment arm on the release bar.</u>

Free body diagram (FBD)

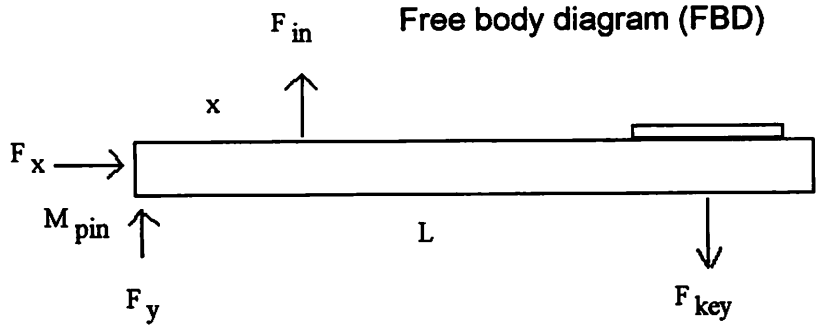

Sum moments about the pin:

$-F_{in} \cdot x + F_{key} \cdot L_{arm} = 0$

$x := 3, 3.01 .. 10$ Range of x values that would be acceptable

$L_{arm} := 14 \cdot in$ Fix the length (L) to be 14 inches

$F_{key} = F_{in} \cdot \frac{x}{L_{arm}} \cdot in$ Force on the key as a function of x $F_{key}(x) := F_{in} \cdot \frac{x \cdot in}{L_{arm}}$

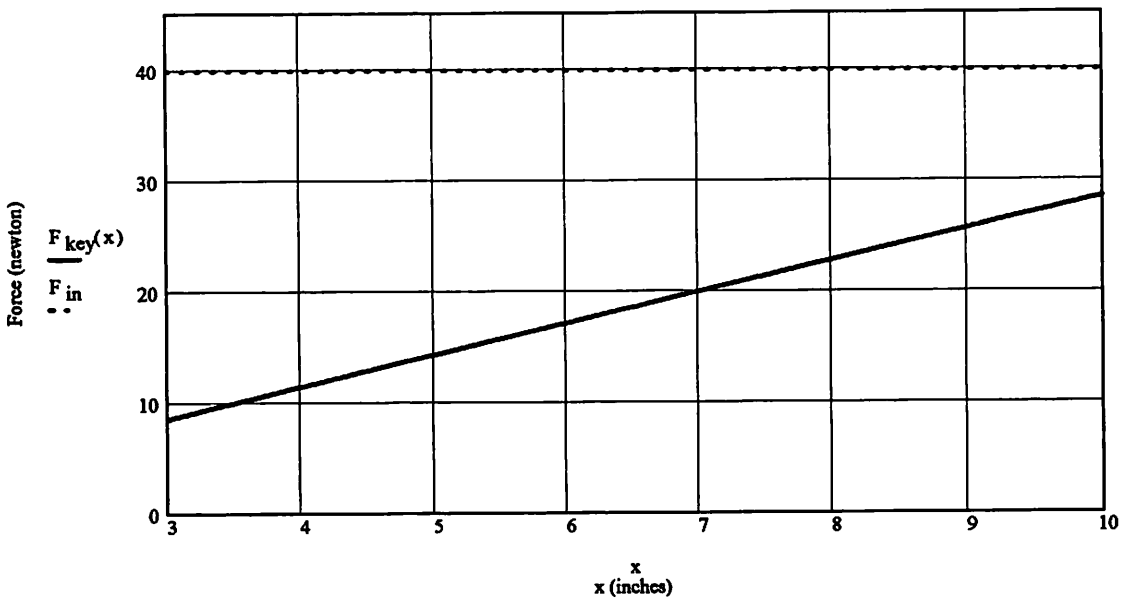

Figure B1: This plot shows that the force on the key approaches the total force as the buoy placement approaches that of the key. A reduction in the force actually supported by the key is desired; so lower x values are desired for the design.

The torque associated with the reduction of the force on the key by varying x was calculated below.

$$F_{key}(x) := \frac{F_{in} \cdot x \cdot in}{L_{arm}} \qquad F_{friction}(x) := \mu_{key} \cdot \left(\frac{F_{key}(x)}{2} \right)$$

Torque on the key is:

$$T_r(x) := \left(F_{friction}(x) \cdot \frac{L_{key}}{2} + F_{friction}(x) \cdot \frac{L_{key}}{2} \right) \cdot 8.851 \quad \text{where} \quad 1 \cdot newton \cdot m = 8.851 \cdot lbf \cdot in$$

$T_{rl} := T \cdot 8.851$ This is the maximum torque required by the solenoid

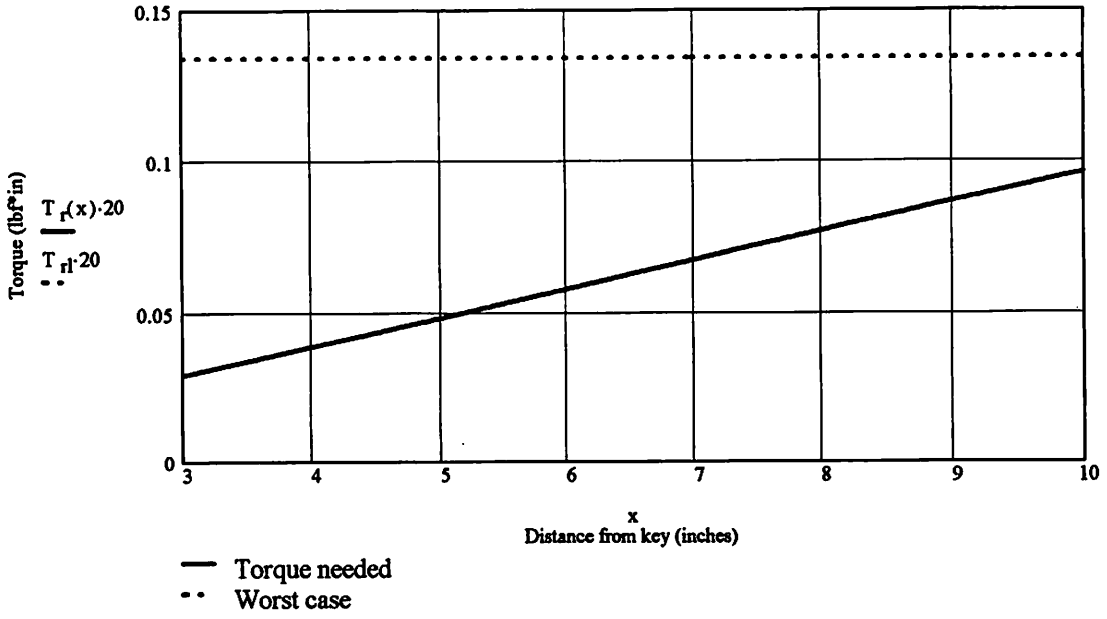

Figure B3: This figure shows the torque with a added safety factor of twenty to garantee that the solenoid can overcame all the friction in the system. The majority of the friction will come from the bearings and or lip seals which prevent water from entering the canister.

Estimate the volume that the retrival line will occupy.

$r_{line} := \frac{1}{8} \cdot in$ Radius of the line

$L_{line} := 1400 \cdot ft$ Length of the line

$V_{line} := \pi \cdot r_{line}^2 \cdot L_{line}$ $V_{line} = 0.477 \cdot ft^3$ $V_{line} = 824.668 \cdot in^3$ Volume of line

Add on thirty percent because a rope cannot be packed perfectly with no gaps.

$V_{line} \cdot 1.3 = 0.62 \cdot ft^3$

Volume of the line that can be expected

$V_{line} \cdot 1.3 = 1072.0685 \cdot in^3$

The estimated size of the holding spool that is needed for the line.

$width := 11 \cdot in$ Width of the spool

$D_{spool} := 11.5 \cdot in$ Diameter of the the spool

$V_{spool} := \pi \cdot \left(\frac{D_{spool}}{2}\right)^2 \cdot width$ Volume of the spool

Comparing the volume of line and the volume of the holding spool it can be seen that the spool has to be quite large but should hold the required amount of line.

$V_{spool} = 1142.558 \cdot in^3$ $V_{line} \cdot 1.3 = 1072.0685 \cdot in^3$

$V_{spool} > V_{line} \cdot 1.3$

Appendix C

Pressure Vessel Analysis

Appendix C:

Analysis of the pressure vessel (Hayden Turner)

$\rho := 1026 \cdot \frac{kg}{m^3}$ density of seawater $d := 1400 \cdot ft$ depth

$P := \rho \cdot g \cdot d$ $P = 622.719 \cdot psi$ pressure at depth d

$h := 5 \cdot in$ height of cylinder

$ri := \frac{7}{2} \cdot in$ inner radius $k := 1 \cdot 10^3$ conversion factor

$ro := \frac{8}{2} \cdot in$ outer radius

$t := ro - ri$ thickness of canister

Hoop Stress Analysis for thin walled cylinders

$\sigma_r(r_1) := \frac{P \cdot r_1}{t}$ Radial stress

$r_1 := ri, ri + 0.1 \cdot in .. ro$ Range variable

$\sigma_t(r_1) := \frac{P \cdot r_1}{2 \cdot t}$ Tangential stress

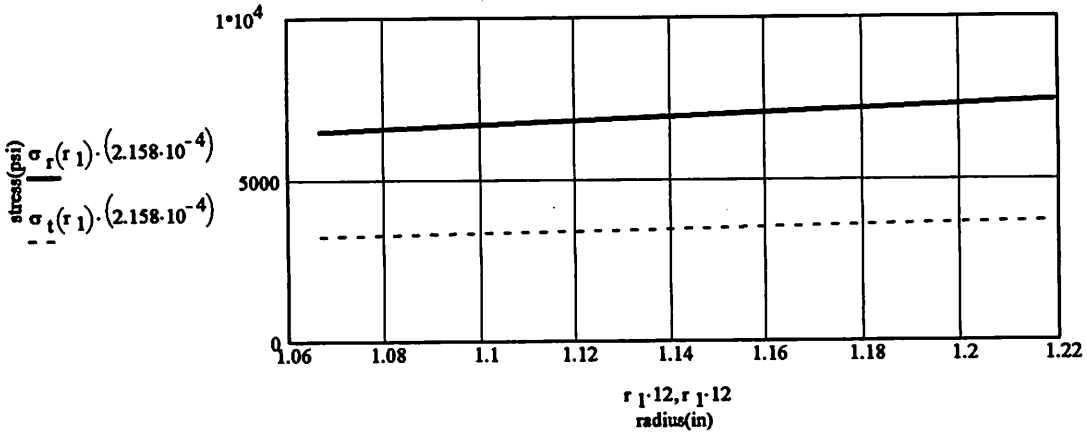

Figure C1: This figure shows the tangential and radial stresses in the canister using thin walled cylinder analysis. The stress values are no where near the yield strength of aluminum.

Thick walled cylinder analysis

$p_i := 1 \cdot atm$ inner pressure

$p_o := P$ Outer pressure

$1 \cdot \frac{kg}{m \cdot sec^2} = 1.45 \cdot 10^{-4} \cdot psi$ Conversion factor

$$\sigma_t(r_1) := \frac{p_i \cdot ri^2 - p_o \cdot ro^2 - ri^2 \cdot ro^2 \cdot \frac{p_o - p_i}{r_1^2}}{ro^2 - ri^2}$$ Tangential stress

$$\sigma_r(r_1) := \frac{p_i \cdot ri^2 - p_o \cdot ro^2 + (ri^2 \cdot ro^2) \cdot \frac{p_o - p_i}{r_1^2}}{ro^2 - ri^2}$$ Radial stress

$S_y := 40 \cdot k \cdot psi$ Yield strength of Aluminium

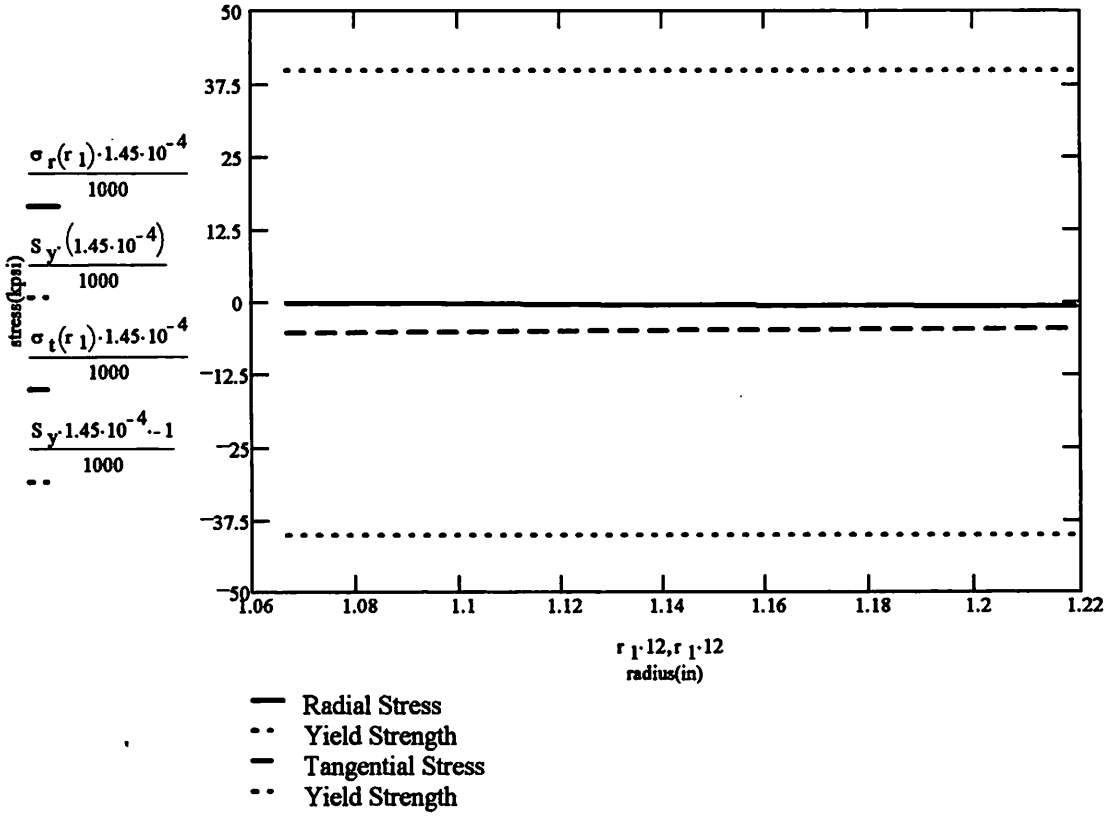

Figure C2: The plot above shows that the stresses in the canister are well within the range of yield stress so the canister will not fail.

$$Safety\_factor := \left| \frac{S_y}{\sigma_t(ri)} \right|$$ $Safety\_factor = 7.688$

Check to see if the canister will fail in buckling

$E := 10.3 \cdot 10^6 \cdot psi$ Modulus of Elasticity

$\nu := 0.33$ Poisons Ratio

$t_p := 1 \cdot in$ Thickness of the cap or plate

$\delta_r := \frac{P \cdot (ri + 0.25 \cdot in)^2}{E \cdot t}$ $\delta_r = 1.7 \cdot 10^{-3} \cdot in$ Radial diflection of the canister

$D := \frac{E \cdot t_p^3}{12 \cdot (1 - \nu^2)}$ Ridgitity of the plate

$\delta_p := \frac{P \cdot ro^4}{D \cdot 64}$ $\delta_p = 2.586 \cdot 10^{-3} \cdot in$ Deflection of the plate at the center

$A_c := 2 \cdot \pi \cdot ro \cdot h$ $A_c = 125.664 \cdot in^2$ Area of the cylinder wall

$F := P \cdot A_c$ $F = 78.253 \cdot k \cdot lbf$ Force on the cylinder wall

$P_{cr} := \frac{E}{4 \cdot \left(\frac{t}{in} - \nu^2\right)} \cdot \frac{t^3}{\left(ri + \frac{t}{2}\right)^3}$ Critical pressure for a unstiffened circular cylinder

$P_{cr} = 1.561 \cdot 10^4 \cdot psi$ $P_{cr} > P$ Therefore the cylinder will not fail in buckling

Appendix D

Solenoid Parameters

Appendix D:

Calculation of solenoid parameters (Hayden Turner, Jud DeCew, Scott Brimlow)

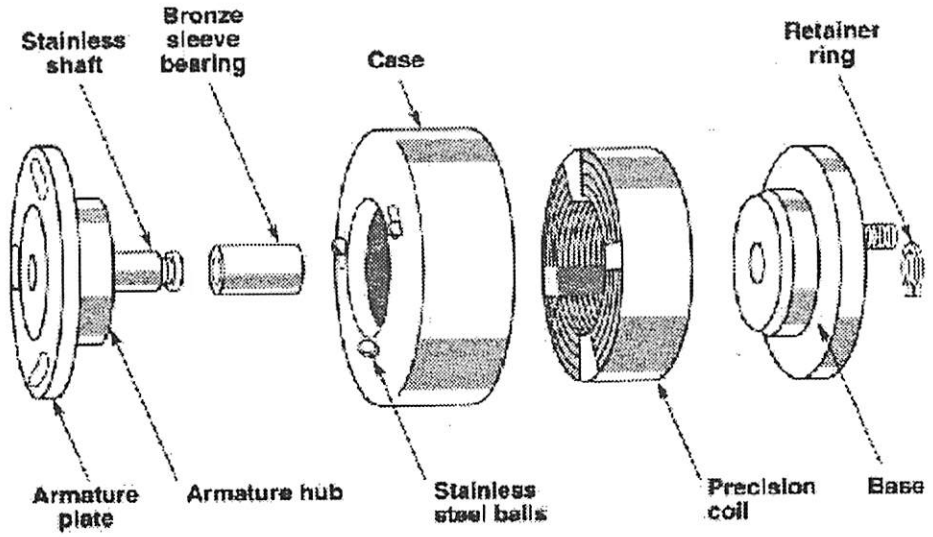

Figure D1: This picture shows an exploded view of the the rotary solenoid.

Find the mass moment of inertia for the test arm on the solenoid.

$L_a := 2.04 \cdot in$ $w_a := .5 \cdot in$ $d_a := .250 \cdot in$

$R_d := \frac{w_a}{2}$ $d_d := .312 \cdot in$ $R_{di} := .188 \cdot in$

Dimensions of each piece

$R_p := R_{di}$ $d_p := .663 \cdot in$

$Area_a := L_a \cdot w_a$ $Area_a = 1.02 \cdot in^2$

Area of each piece

$Area_d := \left(\pi \cdot R_d^2\right) - \left(\pi \cdot R_p^2\right)$ $Area_d = 0.085 \cdot in^2$

$Area_p := \pi \cdot R_p^2$ $Area_p = 0.111 \cdot in^2$

$V_a := Area_a \cdot d_a$ $V_a = 0.255 \cdot in^3$

Volume of each piece

$V_d := Area_d \cdot d_d$ $V_d = 0.027 \cdot in^3$

$V_p := Area_p \cdot d_p$ $V_p = 0.074 \cdot in^3$

$\rho_a := .101 \cdot \frac{lb}{in^3}$ $\rho_a = 2.796 \cdot 10^3 \cdot kg \cdot m^{-3}$

$\rho_d := 0.286 \cdot \frac{lb}{in^3}$ $\rho_d = 7.916 \cdot 10^3 \cdot kg \cdot m^{-3}$ Volume of each piece

$\rho_p := \rho_d$ $\rho_p = 7.916 \cdot 10^3 \cdot kg \cdot m^{-3}$

$m_a := V_a \cdot \rho_a$ $m_a = 0.012 \cdot kg$

$m_d := V_d \cdot \rho_d$ $m_d = 3.453 \cdot 10^{-3} \cdot kg$ Mass of each piece

$m_p := V_p \cdot \rho_p$ $m_p = 9.55 \cdot 10^{-3} \cdot kg$

$J_a := \frac{m_a}{12} \cdot \left(L_a^2 + w_a^2\right)$ $J_a = 2.771 \cdot 10^{-6} \cdot kg \cdot m^2$

$J_d := \frac{m_d}{4} \cdot \left(R_d^2 + R_{di}^2 + \frac{d_d^3}{in}\right)$ $J_d = 7.141 \cdot 10^{-8} \cdot kg \cdot m^2$ Inertia of each piece

$J_p := \frac{m_p \cdot d_p^2}{12}$ $J_p = 2.257 \cdot 10^{-7} \cdot kg \cdot m^2$

Use the parallel axis theorem to find the mass moments of inertia about the axis of rotation

$h_a := \frac{2.04 \cdot in}{2} - .380 \cdot in$ $h_d := 1.379 \cdot in$ $h_p := 1.379 \cdot in$

$J_{ac} := J_a + m_a \cdot h_a^2$ $J_{dc} := J_d + m_d \cdot h_d^2$ $J_{pc} := J_p + m_p \cdot h_p^2$

$J_{tc} := J_{ac} + J_{dc} + J_{pc}$ $J_{tc} = 0.076 \cdot lb \cdot in^2$

Moment of inertia

$I_{ya} := \frac{1}{12} \cdot \left(L_a \cdot w_a^3\right)$ $I_{yd} := \frac{\pi}{4} \cdot \left(R_d^4 - R_{di}^4\right)$ $I_{yp} := \frac{\pi \cdot R_p^4}{4}$

Use the parallel axis theorem to find the mass moments of inertia about the axis of rotation

$h_a := \frac{2.04 \cdot in}{2} - .380 \cdot in$ $h_d := 1.379 \cdot in$ $h_p := 1.379 \cdot in$

$I_{yac} := I_{ya} + Area_a \cdot h_a^2$ $I_{ydc} := I_{yd} + Area_d \cdot h_d^2$ $I_{ypc} := I_{yp} + Area_p \cdot h_p^2$

$I_{yac} = 0.439 \cdot in^4$ $I_{ydc} = 0.164 \cdot in^4$ $I_{ypc} = 0.212 \cdot in^4$

$I_{yt} := I_{yac} + I_{ydc} + I_{ypc}$ $I_{yt} = 0.815 \cdot in^4$

Resistance torque caused by the arm

$T := \left(m_a \cdot d_a + m_d \cdot d_d + m_p \cdot d_p\right) \cdot g$

$T = 0.023 \cdot lbf \cdot in$

Estimate the mass moment of the solenoid

Shaft

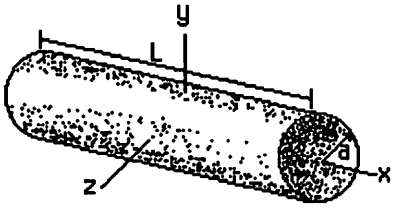

$L_{shaft} := 1.45 \cdot in$ $a_{shaft} := .125 \cdot in$ $specificw_{shaft} := .286 \cdot \frac{lb}{in^3}$

$V_{shaft} := \pi \cdot a_{shaft}^2 \cdot L_{shaft}$ $M_{shaft} := specificw_{shaft} \cdot V_{shaft}$

$I_{xshaft} := \frac{1}{2} \cdot M_{shaft} \cdot a_{shaft}^2$ $I_{xshaft} = 3.433 \cdot 10^{-8} \cdot lbf \cdot ft \cdot sec^2$

Armature Hub

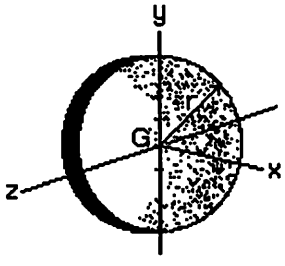

$t_{disk1} := .15 \cdot in$ $r_{disk1} := .875 \cdot in$ $specificw_{disk1} := .286 \cdot \frac{lb}{in^3}$

$V_{disk1} := \pi \cdot r_{disk1}^2 \cdot t_{disk1}$ $M_{disk1} := specificw_{disk1} \cdot V_{disk1}$

$I_{xdisk1} := \frac{1}{2} \cdot M_{disk1} \cdot r_{disk1}^2$

$I_{xdisk1} = 8.526 \cdot 10^{-6} \cdot lbf \cdot ft \cdot sec^2$

Armature Plate

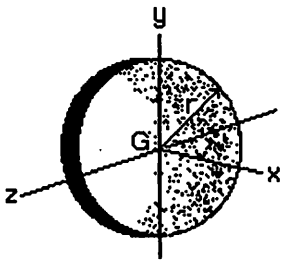

$t_{disk2} := .25 \cdot in$ $r_{disk2} := .5 \cdot in$ $specificw_{disk2} := .286 \cdot \frac{lb}{in^3}$

$V_{disk2} := \pi \cdot r_{disk2}^2 \cdot t_{disk2}$ $M_{disk2} := specificw_{disk2} \cdot V_{disk2}$

$I_{xdisk2} := \frac{1}{2} \cdot M_{disk2} \cdot r_{disk2}^2$ $I_{xdisk2} = 1.515 \cdot 10^{-6}$ $\cdot lbf \cdot ft \cdot sec^2$

$I_{xtotal} := I_{xshaft} + I_{xdisk1} + I_{xdisk2}$ $I_{xtotal} = 0.047 \cdot lb \cdot in^2$

$J_{total} := I_{xtotal} + J_{tc}$

The total mass moment of inertia for the system

$J_{total} = 3.577 \cdot 10^{-5}$ $\cdot kg \cdot m^2$

Electrical model

$i_R = \frac{e_o - e_i}{R}$ $\quad i_L = \frac{e_i}{L \cdot D}$ $\quad i_L = i_R$

$e_0 = i \cdot R_i = i \cdot (1 \cdot ohm)$ Voltage is equal to the current

$e_i = R_t \cdot i + L \cdot \frac{di}{dt}$ Equation of the electrical model

$E_i = (R_t + L \cdot s) \cdot I(s)$ Laplace transform

$$\frac{I(s)}{E_i(s)} = \frac{1}{R_t + L \cdot s} = \frac{\frac{1}{R_t}}{\left(\frac{L}{R_t}\right) \cdot s + 1}$$ Transfer function

$$I(s) = \left(\frac{1}{s}\right) \cdot \left[\frac{\frac{1}{R_t}}{\left(\frac{L}{R_t}\right) \cdot s + 1}\right]$$ Give it an impulse input of 5 volts.

$$i(t) = \frac{1}{R_t} \cdot \left(1 - e^{-\frac{L}{R_t} \cdot t}\right)$$ Function for the current

$R_T := 1.2 \cdot ohm$ Resistance of the circuit

$R_s := 10.6 \cdot ohm$ Resistance of the solenoid

$\tau := 24 \cdot 10^{-3} \cdot sec$ Time constant for the system

$\tau = \frac{L}{R_T}$ Time constant

$L := \tau \cdot R_T$ Solve for the inductance

$L = 0.029 \cdot henry$

$$\frac{I(s)}{E_i(s)} = \frac{1}{R_t + L \cdot s} = \frac{\frac{1}{6 + 4.927 \cdot 10^{-3} \cdot s}}{6}$$ Transfer function

$$\frac{I(s)}{E_i(s)} = \frac{\frac{1}{6}}{\left(\frac{4.927 \cdot 10^{-3}}{6} \cdot s\right) + 1}$$ $\quad \frac{I(s)}{E_i(s)} = \frac{0.167}{8.212 \cdot 10^{-4} \cdot s + 1}$ in standard form

Spring force test

$i := 1..9 \quad ORIGIN := 1$

$$Mass := \begin{bmatrix} 2+\frac{1}{8} \\ 2+\frac{3}{8} \\ 2+\frac{5}{8} \\ 2+\frac{7}{8} \\ 3+\frac{1}{8} \\ 3+\frac{3}{8} \\ 3+\frac{5}{8} \\ 3+\frac{7}{8} \\ 4+\frac{1}{8} \end{bmatrix} \cdot oz$$ Applied mass

Displacement

$$dis_U := \begin{bmatrix} 0.045 \\ 0.098 \\ 0.298 \\ 0.504 \\ 0.617 \\ 0.713 \\ 0.818 \\ 0.844 \\ 0.949 \end{bmatrix} \cdot in \qquad dis_L := \begin{bmatrix} 0 \\ 0.022 \\ 0.041 \\ 0.055 \\ 0.077 \\ 0.176 \\ 0.396 \\ 0.560 \\ 0.710 \end{bmatrix} \cdot in$$

$x := 1.357 \cdot in$ Distance from center of rotation to the measurement distance

Angle of the arm

$$\alpha_{U_i} := atan\left(\frac{dis_{U_i}}{x}\right) \qquad \alpha_{L_i} := atan\left(\frac{dis_{L_i}}{x}\right)$$

$$\alpha_L = \begin{bmatrix} 0 \\ 0.929 \\ 1.731 \\ 2.321 \\ 3.248 \\ 7.39 \\ 16.268 \\ 22.425 \\ 27.619 \end{bmatrix} \cdot deg \qquad \alpha_U = \begin{bmatrix} 1.899 \\ 4.131 \\ 12.386 \\ 20.375 \\ 24.45 \\ 27.719 \\ 31.082 \\ 31.88 \\ 34.967 \end{bmatrix} \cdot deg$$

$$Torque_{mass\_L_i} := \cos\left(\alpha_{L_i}\right) \cdot Mass_i \cdot 1.375 \cdot in \cdot g$$

$$Torque_{mass\_U_i} := \cos\left(\alpha_{U_i}\right) \cdot Mass_i \cdot 1.375 \cdot in \cdot g$$

Torque due to the weight

The effective torque is the torque caused by the arm and corrected due to the change in the rotation angle α.

$$\text{Torque}_{\text{effective\_L}_i} := T \cdot \cos\left(\alpha_{L_i}\right)$$

$$\text{Torque}_{\text{effective\_L}} = \begin{bmatrix} 0.023 \\ 0.023 \\ 0.023 \\ 0.023 \\ 0.023 \\ 0.023 \\ 0.022 \\ 0.021 \\ 0.02 \end{bmatrix} \text{lbf} \cdot \text{in}$$

$$\text{Torque}_{\text{effective\_U}_i} := T \cdot \cos\left(\alpha_{U_i}\right)$$

$$\text{Torque}_{\text{effective\_U}} = \begin{bmatrix} 0.023 \\ 0.023 \\ 0.022 \\ 0.021 \\ 0.021 \\ 0.02 \\ 0.02 \\ 0.019 \\ 0.019 \end{bmatrix} \text{lbf} \cdot \text{in}$$

$$\text{Torque}_{\text{total\_L}_i} := \text{Torque}_{\text{effective\_L}_i} + \text{Torque}_{\text{mass\_L}_i}$$

The total torque

$$\text{Torque}_{\text{total\_U}_i} := \text{Torque}_{\text{effective\_U}_i} + \text{Torque}_{\text{mass\_U}_i}$$

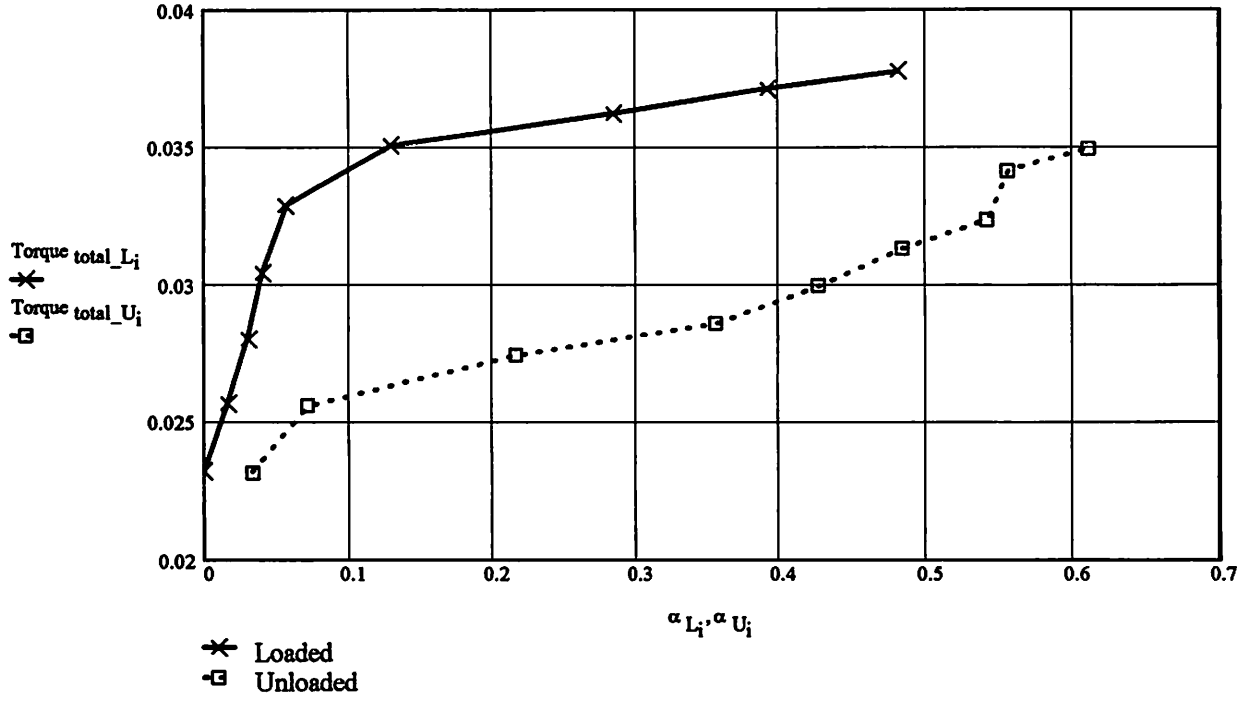

Figure D2: The plot above shows the torque caused by the spring for both the loaded and the unloaded case. The torque due to the arm was subtracted. The slope of the line yields the spring constant.

$T_L(\alpha) := 3.412 \cdot 10^{-3} \cdot \frac{lbf \cdot in}{deg} \cdot \alpha + 0.224 \cdot lbf \cdot in$

$T_U(\alpha) := \left(3.641 \cdot 10^{-3}\right) \cdot \frac{lbf \cdot in}{deg} \cdot \alpha + 0.155 \cdot lbf \cdot in$

$T_L(12 \cdot deg) - T_U(12 \cdot deg) = 0.066 \cdot lbf \cdot in$

$T_{friction} := 0.066 \cdot lbf \cdot in$ Friction associated with the solenoid

$K_{spring} := 0.02 \cdot newton \cdot m$ Spring constant for the solenoid

The current requirements for the solenoid

$$Mass := \begin{bmatrix} 0 \\ .5 \\ 1 \\ 1.5 \\ 2 \\ 2.5 \\ 3 \\ 3.5 \\ 4 \end{bmatrix} \cdot oz \qquad Current := \begin{bmatrix} .65 \\ .69 \\ .73 \\ .75 \\ .79 \\ .82 \\ .85 \\ .88 \\ .91 \end{bmatrix} \cdot amp \qquad i := 1..7 \qquad Voltage := Current \cdot R_s \qquad Voltage = \begin{bmatrix} 6.89 \\ 7.314 \\ 7.738 \\ 7.95 \\ 8.374 \\ 8.692 \\ 9.01 \\ 9.328 \\ 9.646 \end{bmatrix} \cdot volt$$

$m_1 := slope(Mass, Current)$ $m_1 = 0.064 \cdot \frac{amp}{oz}$ $b := intercept(Mass, Current)$ $b = 0.658 \cdot amp$

$M(x) := m_1 \cdot x + b$ Best fit line

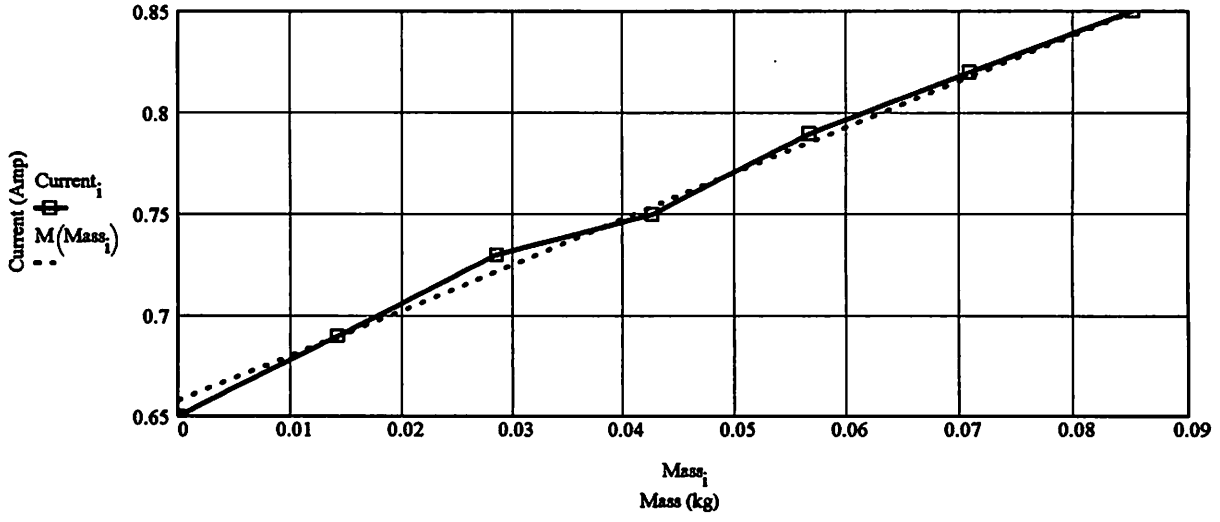

Figure D3: This plot shows how much current is required to turn the solenoid with a specified mass attatched to a test arm.

Torque created by the solenoid

arm := x Torque := Mass·arm·g

$m_3 := \text{slope}(\text{Voltage}, \text{Torque})$ $m_3 = 0.125 \cdot \frac{\text{lbf}\cdot\text{in}}{\text{volt}}$ $m_3 = 0.014 \cdot \frac{\text{newton}\cdot\text{m}}{\text{volt}}$

Best fit

$b_3 := \text{intercept}(\text{Voltage}, \text{Torque})$ $b_3 = -0.868 \cdot \text{lbf}\cdot\text{in}$ $M_3(x) := m_3 \cdot x + b_3$

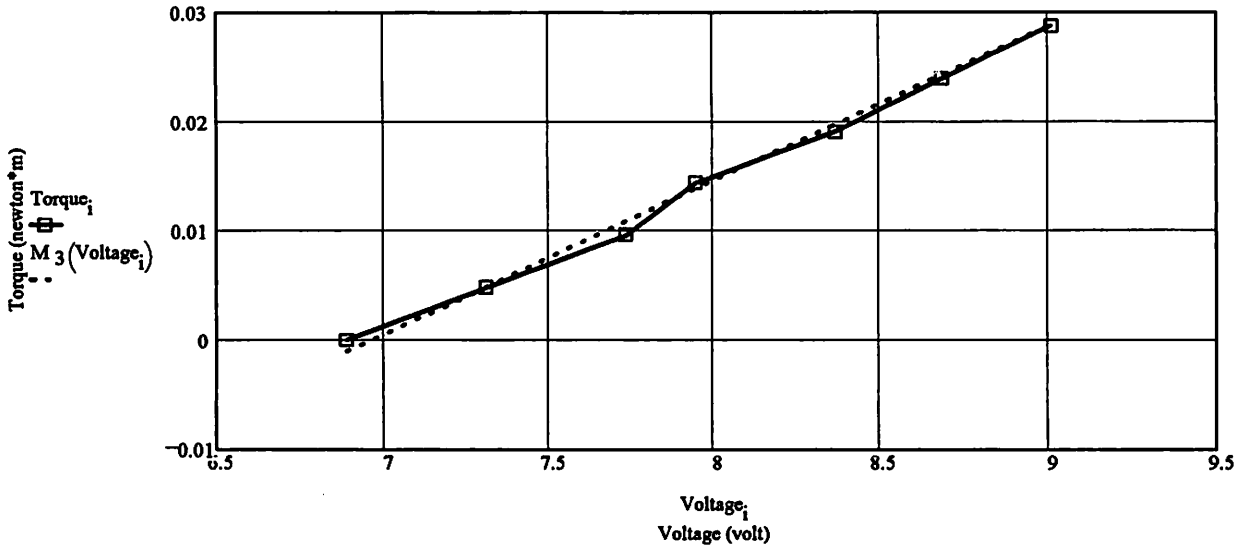

Figure D4: This plot shows the amount of torque applied by the solenoid as a function of voltage.

$\text{Power}_i := (\text{Current}_i)^2 \cdot R_s$ Power requirements

$$\text{Power} = \begin{bmatrix} 4.479 \\ 5.047 \\ 5.649 \\ 5.962 \\ 6.615 \\ 7.127 \\ 7.658 \end{bmatrix} \cdot \text{watt} \qquad \text{Power} = \begin{bmatrix} 15.281 \\ 17.22 \\ 19.274 \\ 20.345 \\ 22.573 \\ 24.32 \\ 26.132 \end{bmatrix} \cdot \frac{\text{BTU}}{\text{hr}}$$

Power requirements

$b_3 = -0.868 \cdot \text{lbf}\cdot\text{in}$

The resistance torque of the solenoid and the arm

$b_3 = -0.098 \cdot \text{newton}\cdot\text{m}$

$K_{\text{torque\_a}} := \text{slope}(\text{Current}, \text{Torque})$ $K_{\text{torque\_a}} = 0.149 \cdot \frac{\text{newton}\cdot\text{m}}{\text{amp}}$ $K_{\text{torque\_v}} := \frac{0.024 \cdot \text{newton}\cdot\text{m}}{\text{volt}}$

Mechanical Model for the solenoid (spring,mass,damper system)

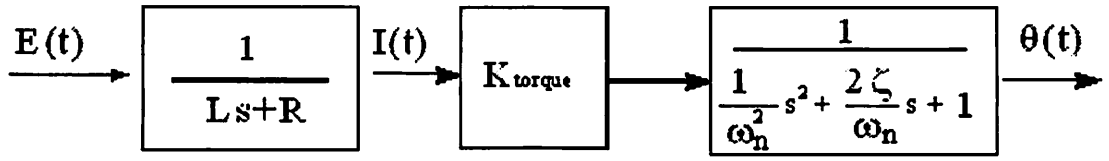

Figure D5: This shows the block diagram of the rotary solenoid.

$R := R_s \qquad G := 4.77 \cdot volt$

$$\left(J \cdot x'' + B \cdot x' + K_{spring} \cdot x\right) = \frac{K_{torque\_a} \cdot G \cdot u(t)}{R}$$

Second order differential equation for a rotational spring mass and damper system.

$$\left(J \cdot s^2 + B \cdot s + K_{spring}\right) \cdot x = \frac{K_{torque\_a} \cdot \frac{1}{s} \cdot G}{R}$$

Transfer function

$$x = \frac{K_{torque\_a}}{s \cdot \left[R \cdot \left(J \cdot s^2 + B \cdot s + K_{spring}\right)\right]}$$

$$\omega_n := \sqrt{\frac{K_{spring}}{J_{total}}}$$

Natural frequency

$$\omega_n = 23.646 \cdot Hz$$

$$x = \frac{\frac{K_{torque\_a}}{R \cdot K_{spring}}}{s \cdot \left(\frac{J}{K_{spring}} \cdot s^2 + \frac{B}{K_{spring}} \cdot s + 1\right)}$$

$$\frac{B}{K_{spring}} = \frac{2 \cdot \zeta}{\omega_n}$$

Damping

$$x = \frac{\frac{K_{torque\_a}}{R \cdot K_{spring}}}{s \cdot \left(\frac{1}{\omega_n^2} \cdot s^2 + \frac{2 \cdot \zeta}{\omega_n} \cdot s + 1\right)} \qquad B = 2 \cdot \zeta \cdot \frac{K_{spring}}{\omega_n}$$

$mili := 1 \cdot 10^{-3}$

$t := 30.7867 \cdot mili \cdot sec$

$x := 45 \cdot deg$

This time t is the time taken for the solenoid to rotate its full rotation angle of 45 degrees.

Find the damping ratio:

$\zeta := .4$ guess or seed

Given

$$x = \left[\frac{K_{torque\_a}}{(R \cdot K_{spring})} \cdot G - G \cdot K_{torque\_a} \cdot \zeta \cdot \exp\left(-\zeta \cdot \omega_n \cdot t\right) \cdot \frac{\sinh\left(\omega_n \cdot \sqrt{-1+\zeta^2} \cdot t\right)}{\left[R \cdot \left(K_{spring} \cdot \sqrt{-1+\zeta^2}\right)\right]} \right] + 0 \ldots$$
$$+ \left[-1 \cdot \left[G \cdot K_{torque\_a} \cdot \exp\left(-\zeta \cdot \omega_n \cdot t\right) \cdot \frac{\cosh\left(\omega_n \cdot \sqrt{-1+\zeta^2} \cdot t\right)}{(R \cdot K_{spring})} \right] \right]$$

$ans := Find(\zeta)$ $ans = 0.171$

$\zeta := 0.171$ Damping Ratio for the mechanical model

$$B := 2 \cdot \zeta \cdot \frac{K_{spring}}{\omega_n}$$

$B = 2.56 \cdot 10^{-3}$ $\cdot lbf \cdot in \cdot sec$ Damping conststant for the mechanical model

Transfer functions for the mechanical and electrical parts

Electrical	Mechanical
$TF_E = \frac{1}{0.029 \cdot s + 10.6}$	$x = \frac{0.704}{s \cdot \left(1.788 \cdot 10^{-3} \cdot s^2 + 0.014 \cdot s + 1\right)}$

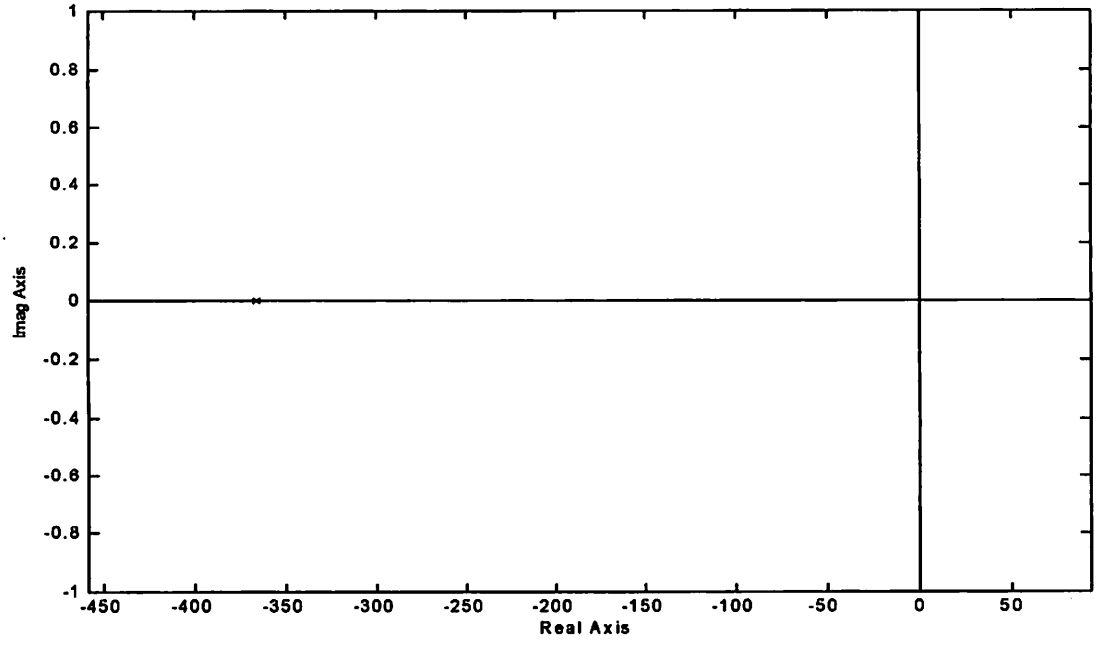

(a)

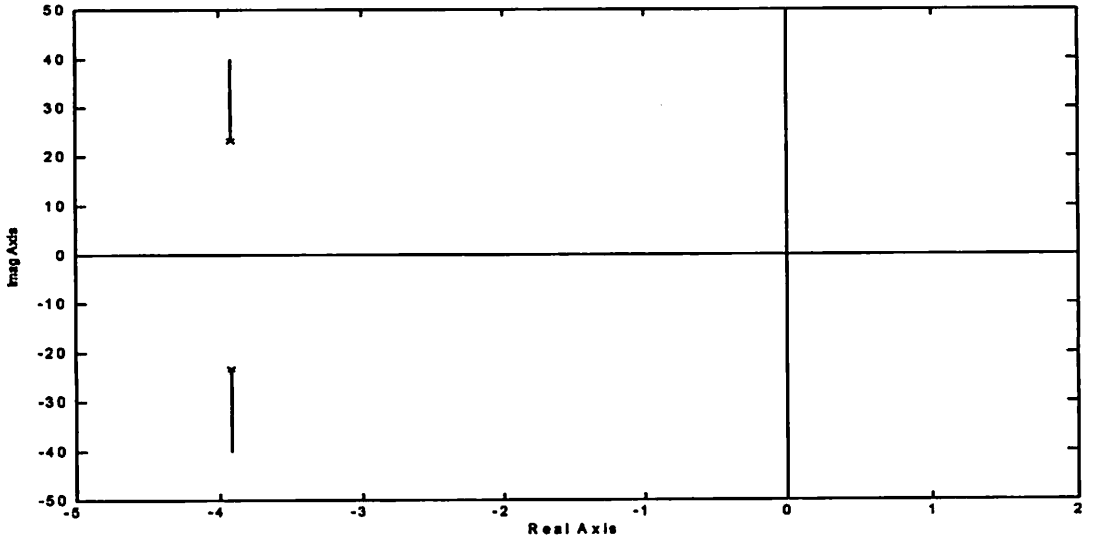

(b)

Figure D6: This plot shows the root locus plot for the electrical model of the rotary solenoid: a) electical b) mechanical

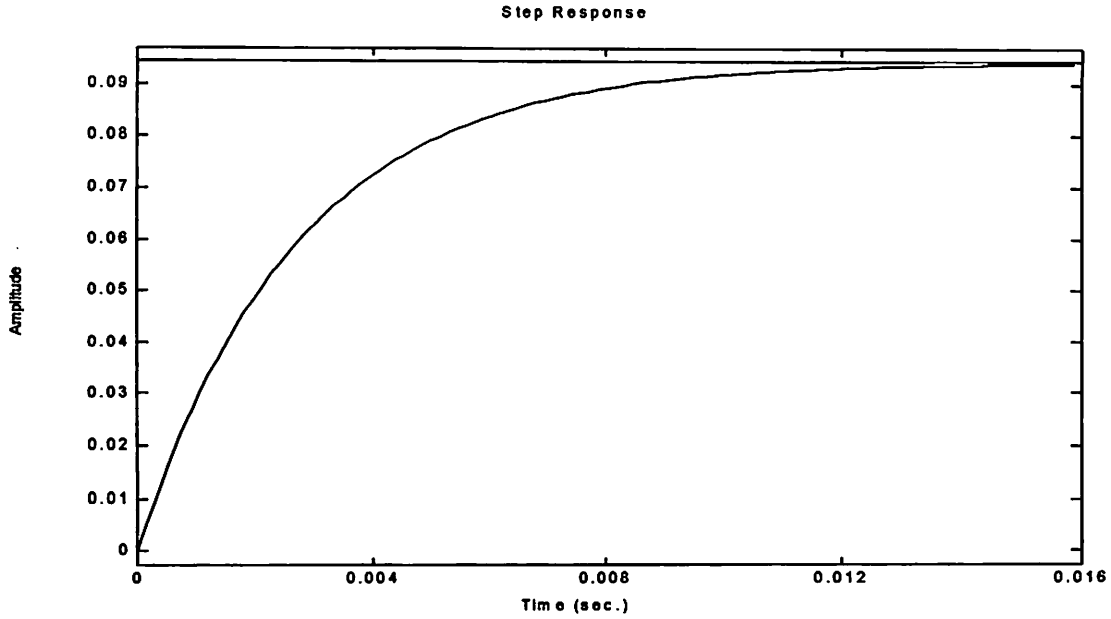

(a)

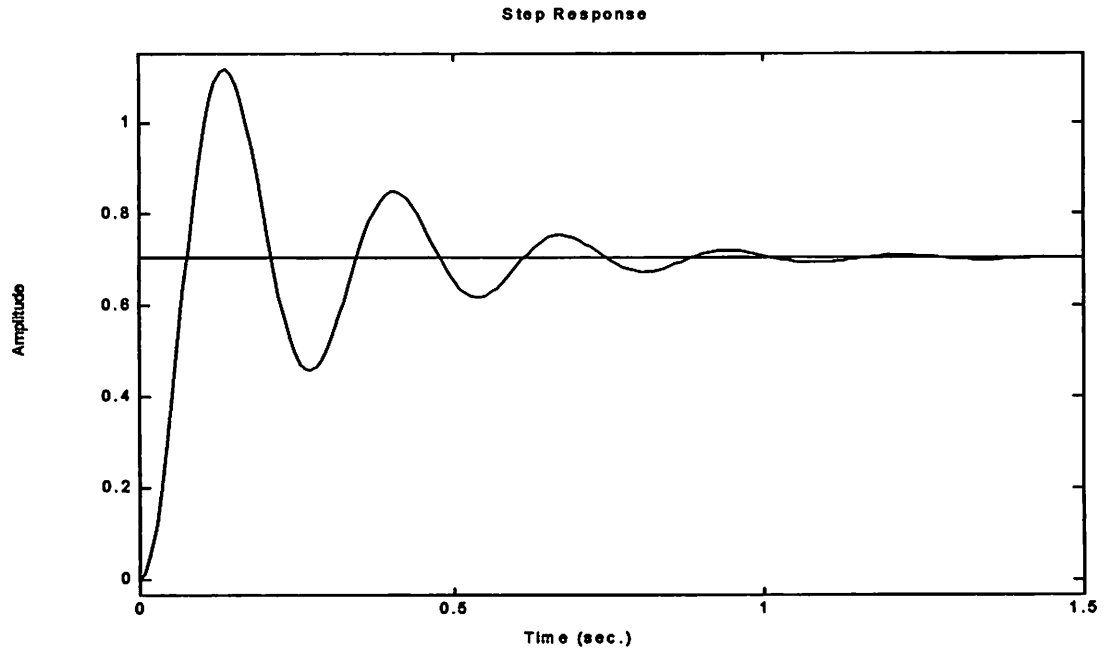

(b)

Figure D7: These plots show the step response for the rotary solenoid: a) electrical b) mechanical

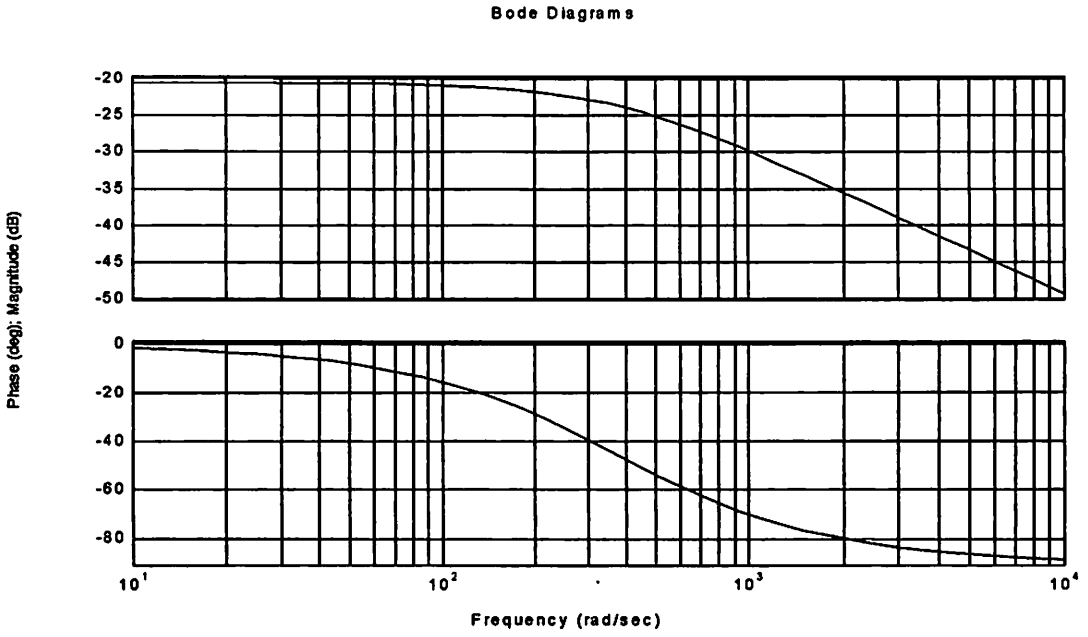

(a)

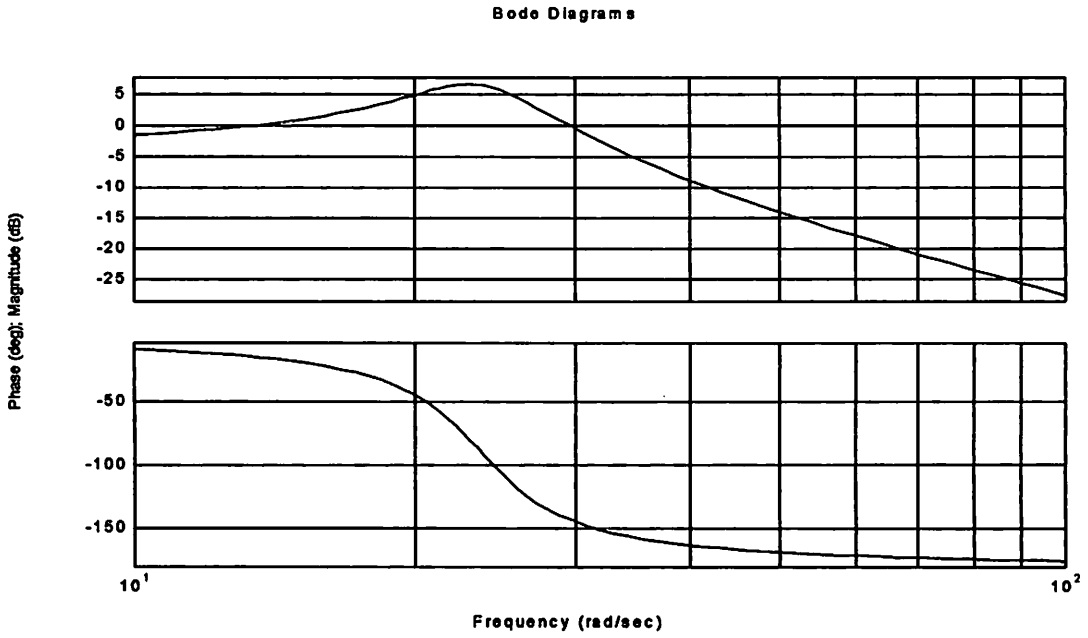

(b)

Figure E6: This figure shows the bode plot for the rotary solenoid: a) electrical part of the system b) mechanical part of the system. Both the phase and the magnitude are plotted against the frequency.

Solenoid parameters

Mechanical

Mass moment of inertia	$J_{total} = 3.577 \cdot 10^{-5} \cdot kg \cdot m^2$
	$J_{total} = 3.166 \cdot 10^{-4} \cdot lbf \cdot in \cdot sec^2$
Spring constant	$K_{spring} = 3.491 \cdot 10^{-4} \cdot newton \cdot \frac{m}{deg}$
	$K_{spring} = 3.089 \cdot 10^{-3} \cdot lbf \cdot \frac{in}{deg}$
Damping ratio	$\zeta = 0.171$
Damping constant	$B = 5.049 \cdot 10^{-6} \cdot newton \cdot m \cdot \frac{sec}{deg}$
	$B = 4.468 \cdot 10^{-5} \cdot lbf \cdot \frac{in \cdot sec}{deg}$
Torque due to friction	$T_{friction} = 7.457 \cdot 10^{-3} \cdot newton \cdot m$
	$T_{friction} = 0.066 \cdot lbf \cdot in$

Electo-mechanical:

Torque constant with respect to current	$K_{torque\_a} = 1.321 \cdot lbf \cdot \frac{in}{amp}$
	$K_{torque\_a} = 0.149 \cdot newton \cdot \frac{m}{amp}$
Torque constant with respect to voltage	$K_{torque\_v} = 0.212 \cdot lbf \cdot \frac{in}{volt}$
	$K_{torque\_v} = 0.024 \cdot newton \cdot \frac{m}{volt}$

Electical:

Resistance	$R_s = 10.6 \cdot ohm$
Inductance	$L = 0.029 \cdot henry$
Time constant	$\tau = 24 \cdot mili \cdot sec$

Appendix E

Mechanical Drawings

PROJECT: BLT

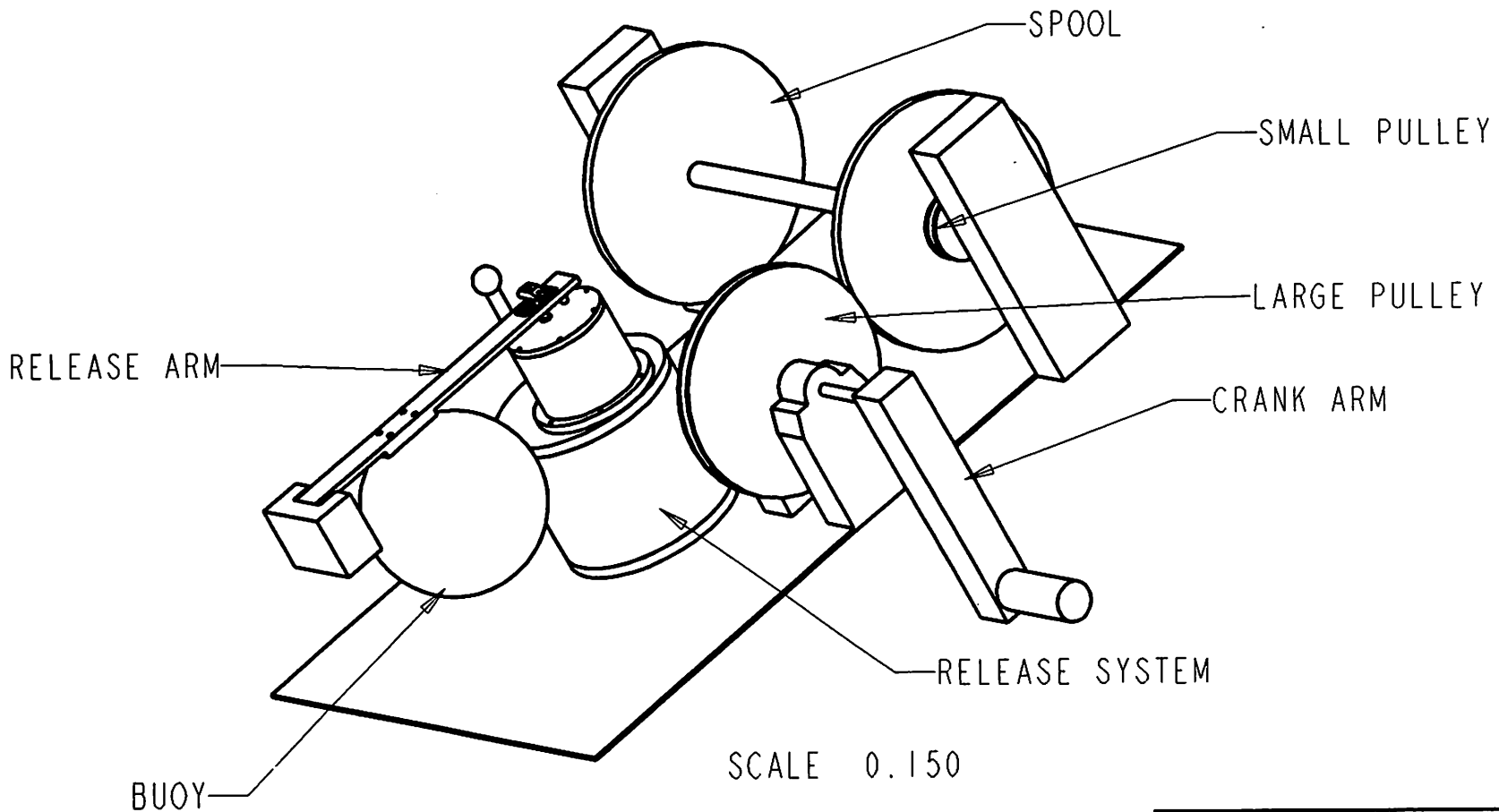

SCALE 0.150

		QUANTITY
UNH MECHANICAL ENGINEERING TECH 797 SENIOR DESIGN	PART	MATERIAL
		UNITS: INCHES
CREATED BY: HAYDEN TURNER	SYSTEM	PROPRIETARY DOCUMENT

PROJECT: BLT

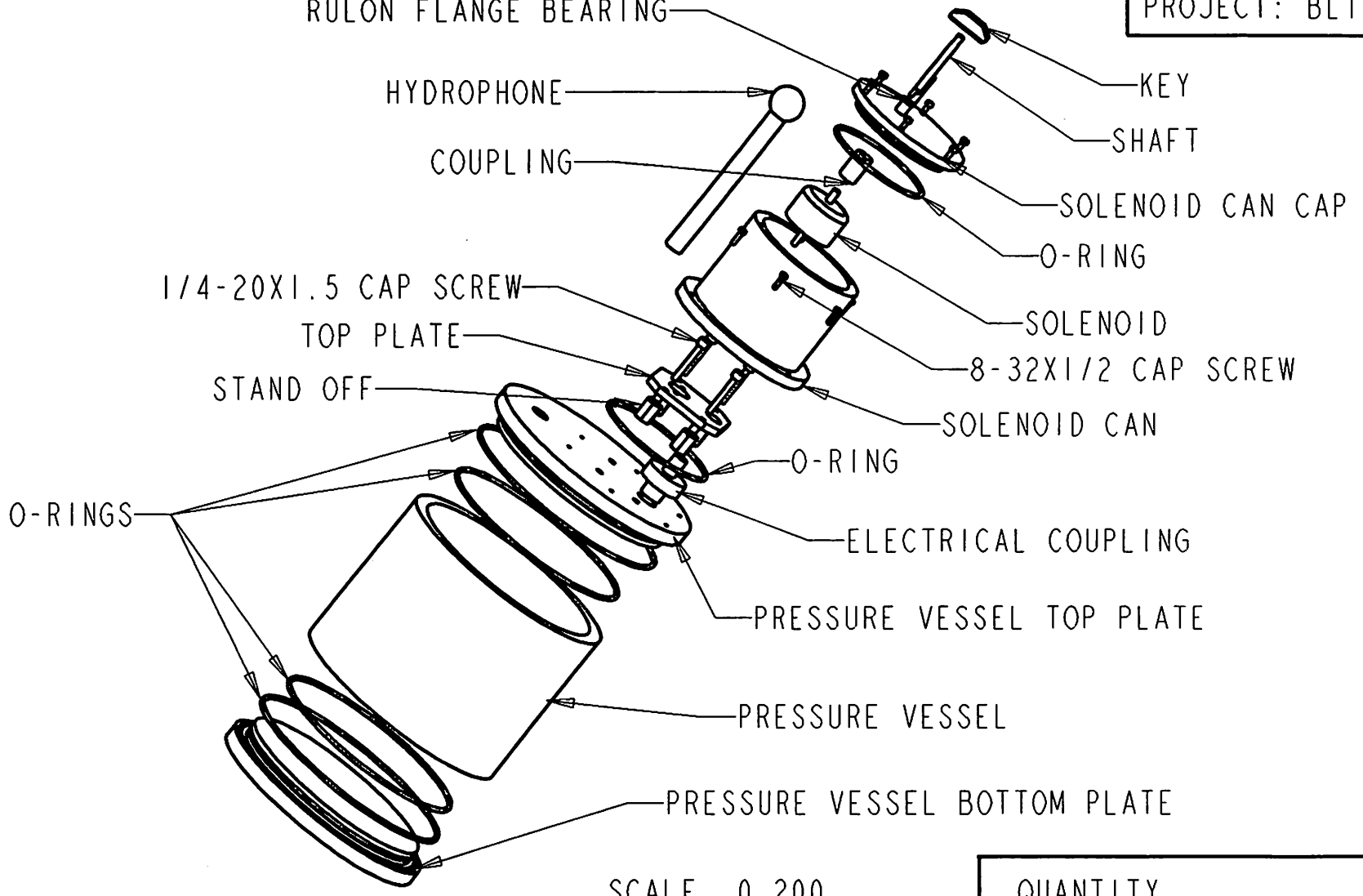

SCALE 0.200

QUANTITY

UNH MECHANICAL ENGINEERING TECH 797 SENIOR DESIGN	PART	MATERIAL
	SYSTEM	UNITS: INCHES
CREATED BY: HAYDEN TURNER		PROPRIETARY DOCUMENT

PROJECT: BLT

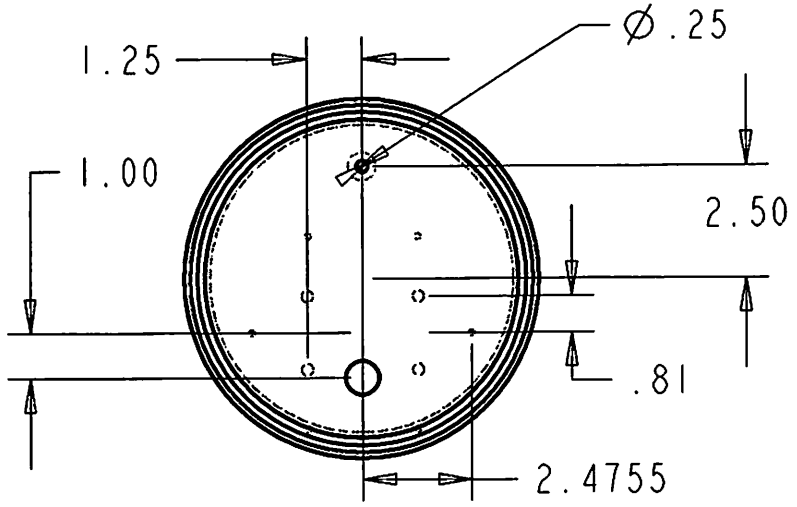

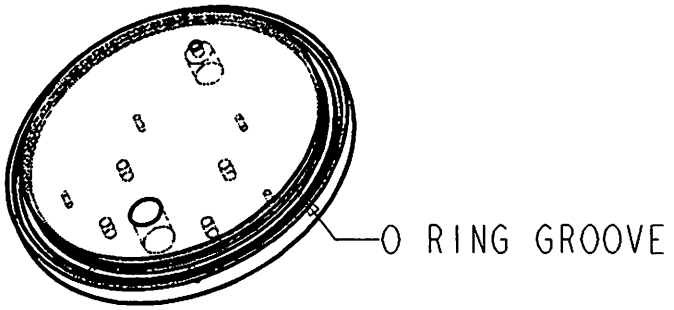

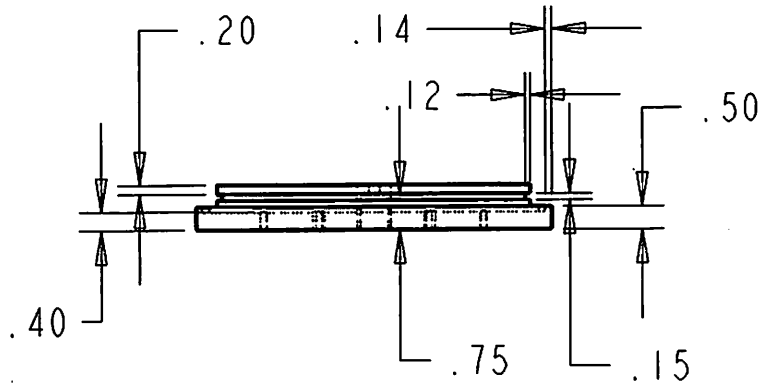

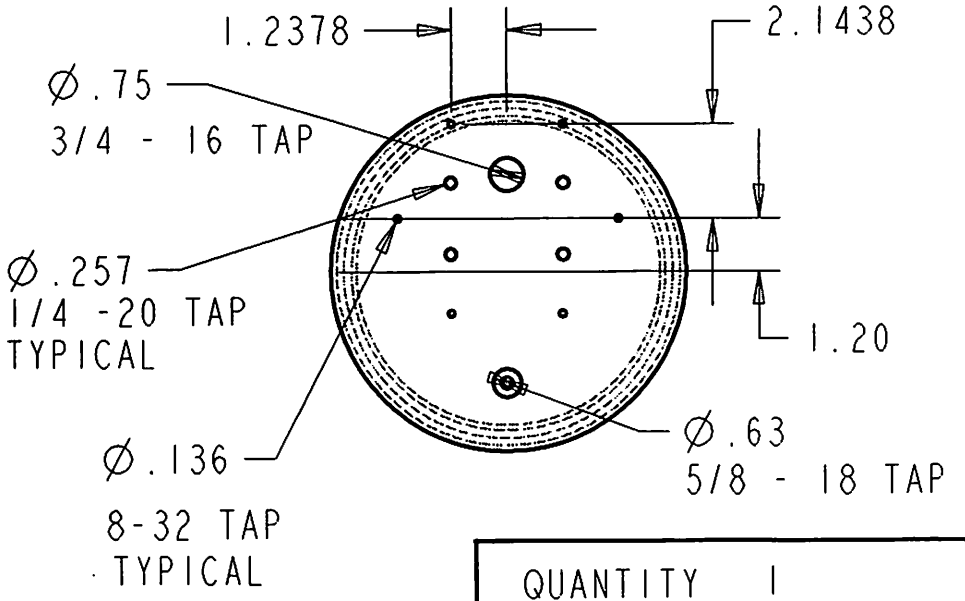

QUANTITY 1

UNH MECHANICAL ENGINEERING TECH 797 SENIOR DESIGN	PART PRESSURE VESSEL TOP PLATE	MATERIAL ALUMINUM
		UNITS: INCHES
CREATED BY: HAYDEN TURNER	SYSTEM RELEASE	PROPRIETARY DOCUMENT

PROJECT: BLT

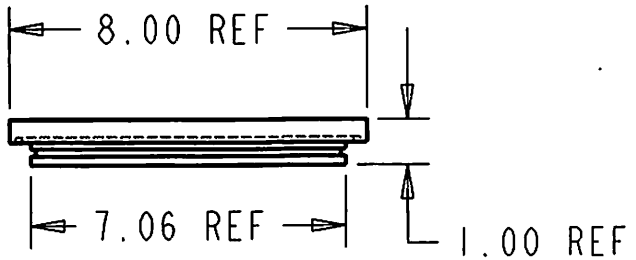

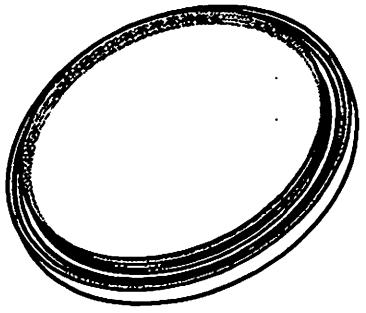

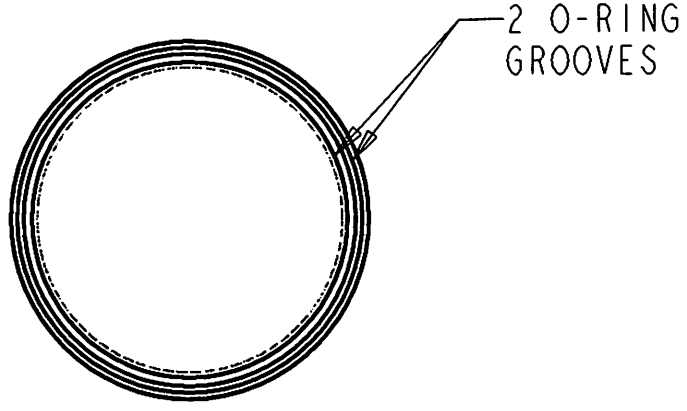

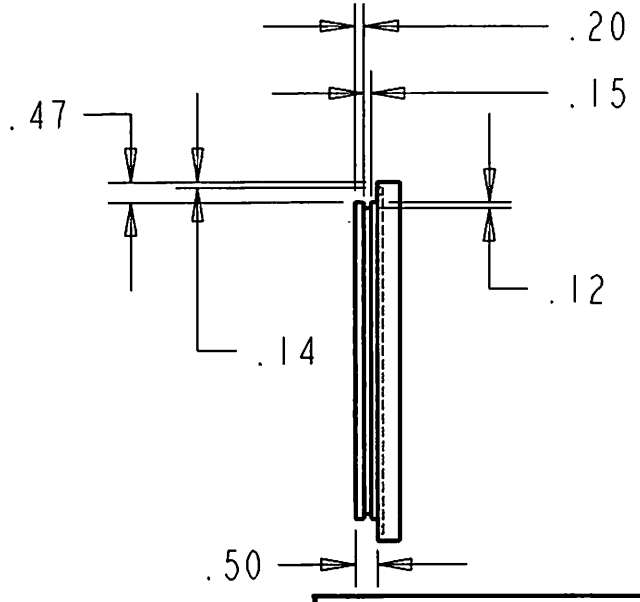

QUANTITY 1

UNH MECHANICAL ENGINEERING TECH 797 SENIOR DESIGN	PART PRESSURE VESSEL BOTTOM PLATE	MATERIAL ALUMINUM
		UNITS: INCHES
CREATED BY: HAYDEN TURNER	SYSTEM RELEASE	PROPRIETARY DOCUMENT

PROJECT: BLT

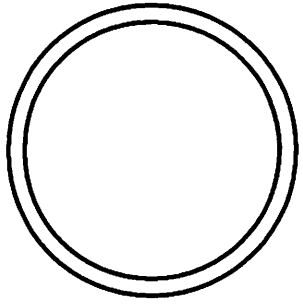

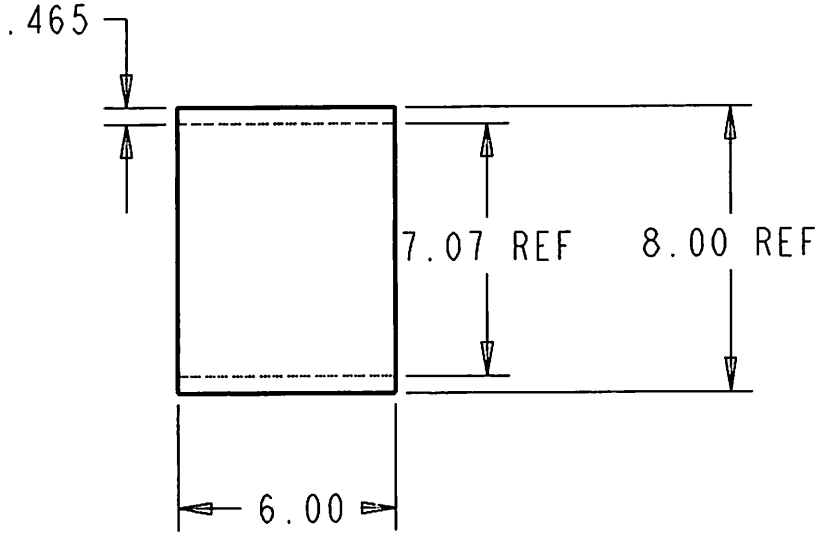

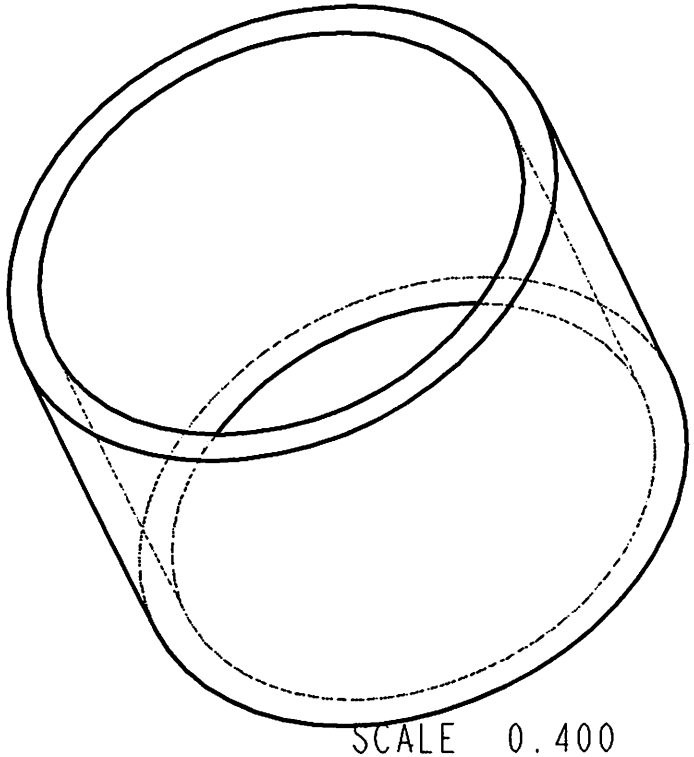

QUANTITY 1

UNH MECHANICAL ENGINEERING TECH 797 SENIOR DESIGN	PART PRESSURE VESSEL	MATERIAL ALUMINUM
		UNITS: INCHES
CREATED BY: HAYDEN TURNER	SYSTEM RELEASE	PROPRIETARY DOCUMENT

PROJECT: BLT

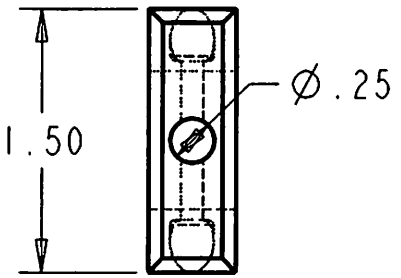

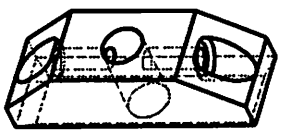

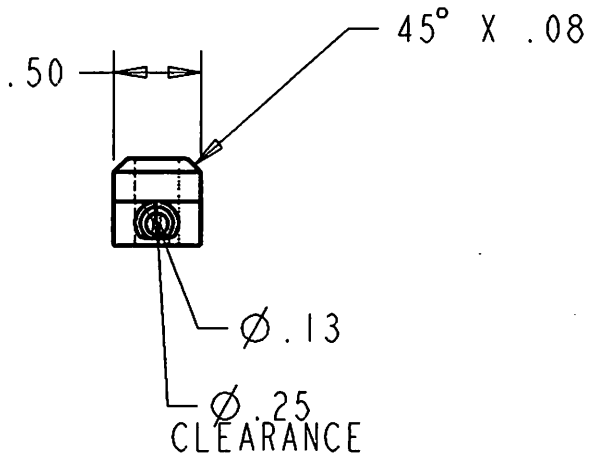

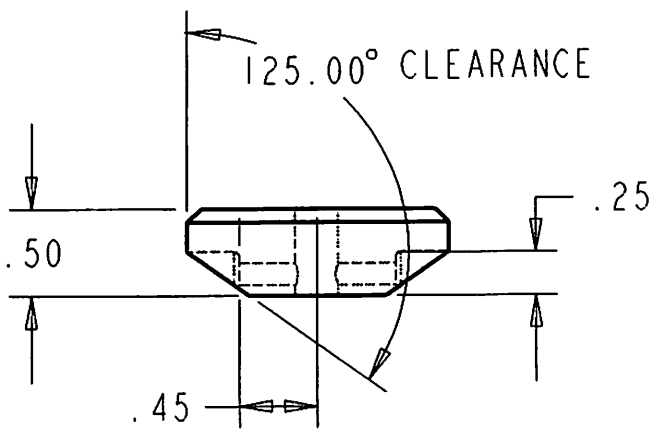

QUANTITY 1

UNH MECHANICAL ENGINEERING TECH 797 SENIOR DESIGN	PART KEY	MATERIAL DELRIN
		UNITS: INCHES
CREATED BY: HAYDEN TURNER	SYSTEM RELEASE	PROPRIETARY DOCUMENT

PROJECT: BLT

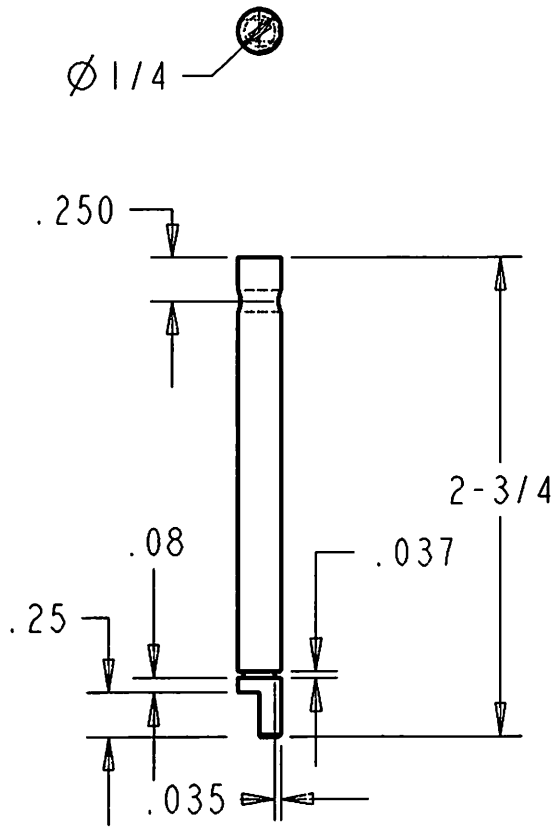

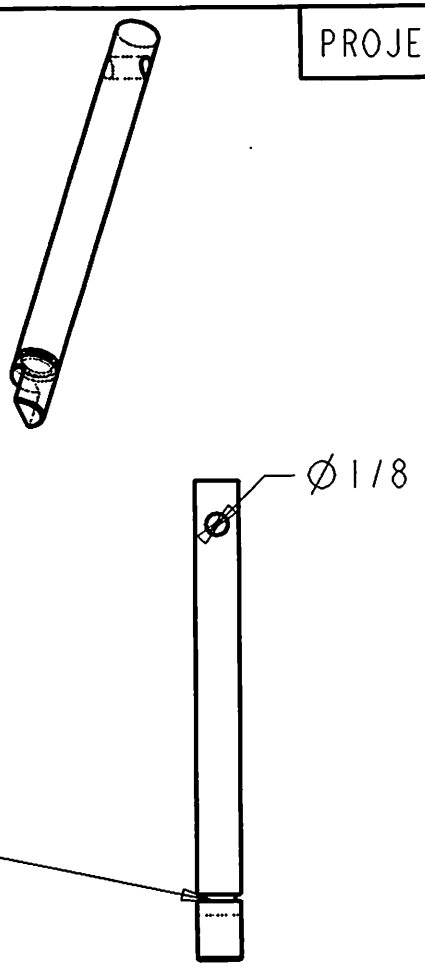

		QUANTITY
UNH MECHANICAL ENGINEERING TECH 797 SENIOR DESIGN	PART SHAFT	MATERIAL STAINLESS STEEL
		UNITS: INCHES
CREATED BY: HAYDEN TURNER	SYSTEM RELEASE	PROPRIETARY DOCUMENT

PROJECT: BLT

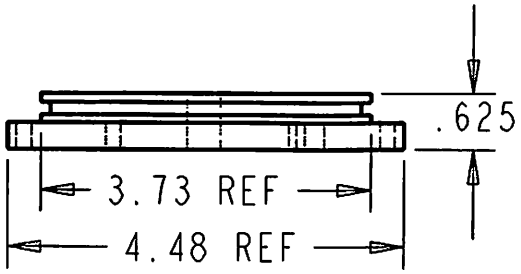

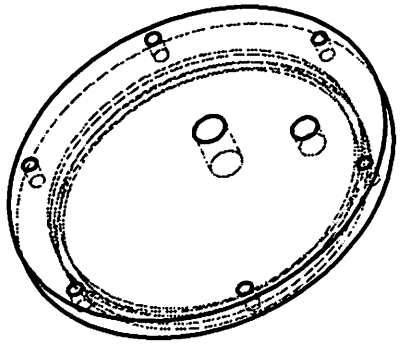

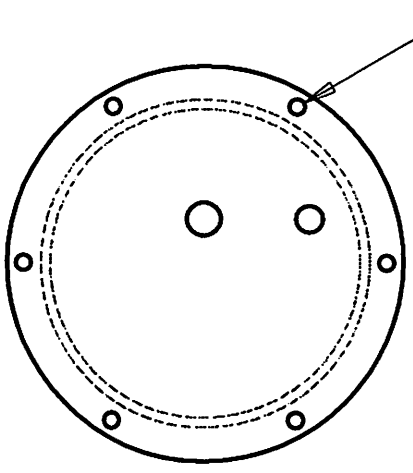

TAP

FOR RETAINING SHAFT

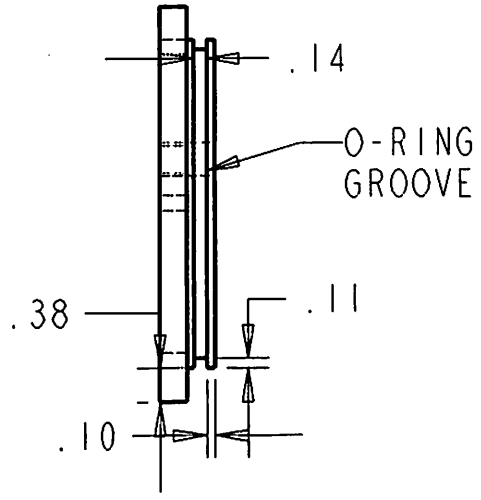

QUANTITY 1

UNH MECHANICAL ENGINEERING TECH 797 SENIOR DESIGN	PART SOLENOID CANISTER CAP	MATERIAL ALUMINUM
		UNITS: INCHES
CREATED BY: HAYDEN TURNER	SYSTEM RELEASE	PROPRIETARY DOCUMENT

PROJECT: BLT

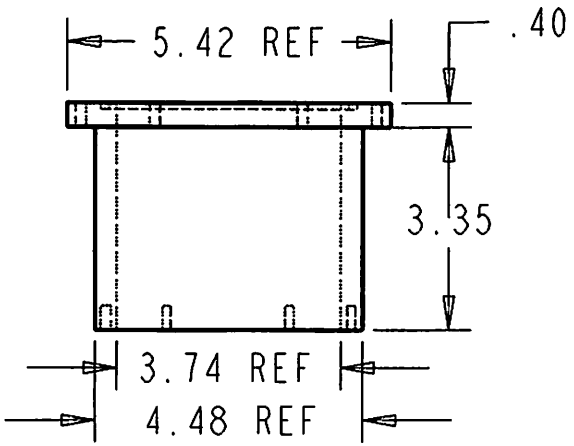

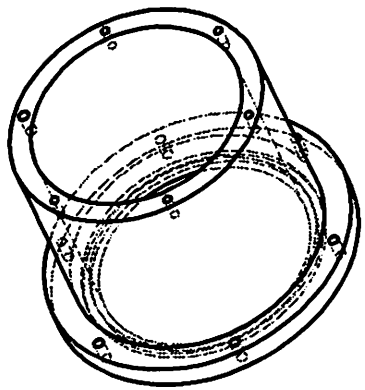

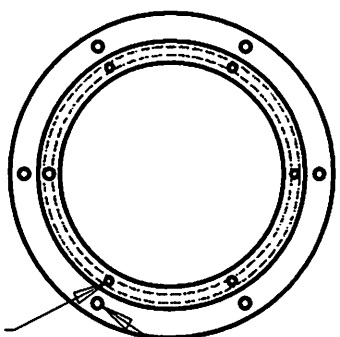

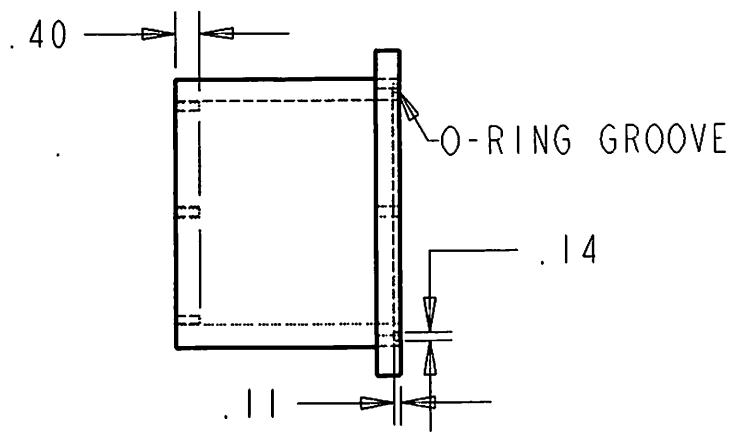

		QUANTITY 1
UNH MECHANICAL ENGINEERING TECH 797 SENIOR DESIGN	PART SOLENOID HOUSING	MATERIAL ALUMINUM
		UNITS: INCHES
CREATED BY: HAYDEN TURNER	SYSTEM RELEASE	PROPRIETARY DOCUMENT

PROJECT: BLT

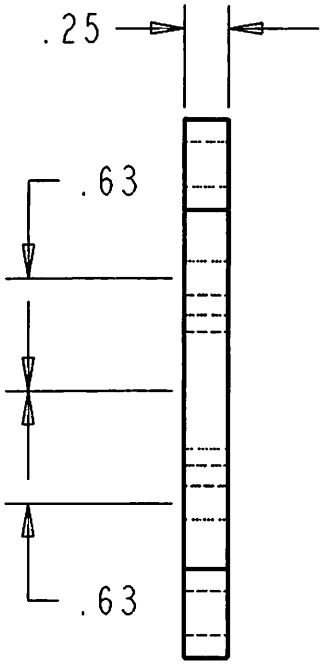

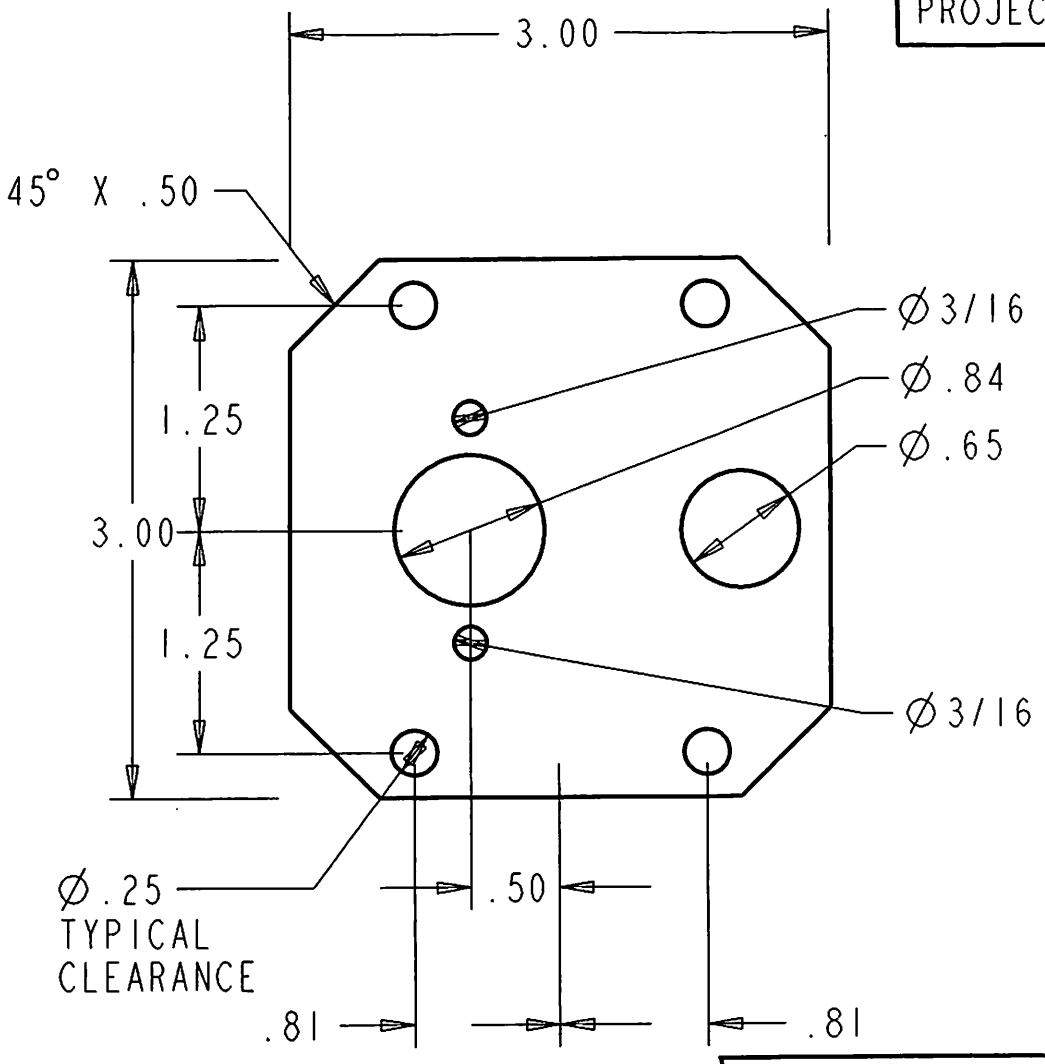

QUANTITY 1

UNH MECHANICAL ENGINEERING TECH 797 SENIOR DESIGN	PART TOP PLATE	MATERIAL ALUMINUM
		UNITS: INCHES
CREATED BY: HAYDEN TURNER	SYSTEM RELEASE	PROPRIETARY DOCUMENT

PROJECT: BLT

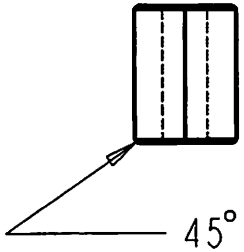

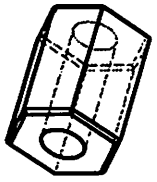

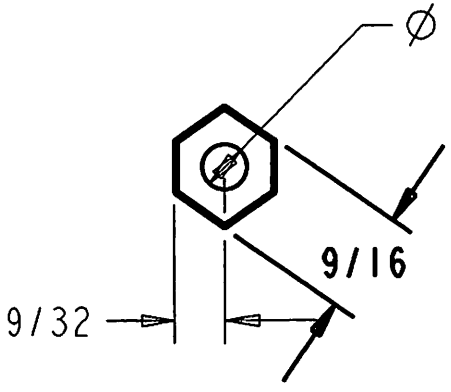

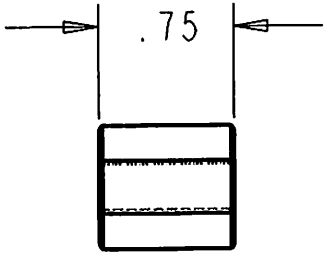

QUANTITY 4

UNH MECHANICAL ENGINEERING TECH 797 SENIOR DESIGN	PART STANDOFF	MATERIAL HEX STOCK
		UNITS: INCHES
CREATED BY: HAYDEN TURNER	SYSTEM RELEASE	PROPRIETARY DOCUMENT

Appendix F

Budget

Appendix F:

Budget (Jud DeCew)

Part	Part Number	Company	Quantity	Cost	Shipping	Total	Details	Component
Rotational Solenoid	H-2617-026	TestCo	1	110	6.52	116.52	Soleniod	Release Mechanism
Delrin	8741K51	McMaster-Carr Su	1	30.31	0	30.31	2" square by 1'	Release Mechanism
Aluminum Plates	89155K47	McMaster-Carr Su	2	36.43	4.81	77.67	Alloy 6061	Release Mechanism
Flange	DRFOR06-4	Applied Industrial	1	5.03	0	5.03	1\4" shaft	Release Mechanism
Bearing	R-4-2RS	Applied Industrial	1	9.8	0	9.8	1/4" shaft	Release Mechanism
Seal	O1-253	Applied Industrial	2	1.2	0	2.4	1/4" shaft	Release Mechanism
Seal	O1-527	Applied Industrial	3	1.4	0	4.2	1/4" shaft	Release Mechanism
Compression Latches	1794A43	McMaster-Carr Su	6	5.25	0	31.5	Spring Draw Latches	Release Mechanism
Batteries		Battery Outlet Inc	12	0.79	5.06	14.54	D-Cell 1.5 volt	Release Mechanism
O-ring	261	Applied Industrial	2	2.5	0	5	6-3/4" by 1/8"	Release Mechanism
O-ring	264	Applied Industrial	2	2.5	0	5	7-1/2" by 1/8"	Release Mechanism
Coupling	60845K31	McMaster-Carr Su	1	22.11	0	22.11	Two-piece	Release Mechanism
Aluminum Plate	8910K152	McMaster-Carr Su	2	32.88	0	65.76	1/4" plate	Release Mechanism
Shaft Seal	9281K65	McMaster-Carr Su	1	7.6	2.76	10.36	SS pump shaft seal	Release Mechanism
U-cup	9691K18	McMaster-Carr Su	1	3.07	0	3.07	Buna-N	Release Mechanism
Shaft Seal	9562K41	McMaster-Carr Su	2	2.82	0	5.64	self adjusting	Release Mechanism
Flange Mount	62645K43	McMaster-Carr Su	1	21.86	0	21.86	2-bolt	Winding Mechanism
V-belt	6186K142	McMaster-Carr Su	1	6.21	0	6.21	44"	Winding Mechanism
Ball Bearing	6357K33	McMaster-Carr Su	2	47.22	0	94.44	Flange Mount - 2 bol	Winding Mechanism
Flange Mount	5912K48	McMaster-Carr Su	2	26.93	0	53.86	.5" Diameter	Winding Mechanism
Flange Mount	62645K43	McMaster-Carr Su	2	21.86	0	43.72	1" Diameter	Winding Mechanism
Aluminum Tubing	8978K76	McMaster-Carr Su	1	11.55	0	11.55	1' Diameter	Winding Mechanism
Pulley	6274K45	McMaster-Carr Su	1	41.15	0	41.15	10" Diameter	Winding Mechanism
Pulley	6274K21	McMaster-Carr Su	1	6.19	0	6.19	3" Diameter	Winding Mechanism
Ball Bearing	6357K11	McMaster-Carr Su	2	38.4	0	76.8	Base Mount - 2 bolt	Winding Mechanism
Misellaneous	-----	Radio Shack	1	62.5	0	62.5	Many small items	Electronics
Misellaneous	-----	Radio Shack	1	19.12	0	19.12	Many small items	Electronics
Op-amp / Comparitor	-----	EE Dept	2	1.5	0	3	Main Assemble	Electronics
Lobster Trap	LB-30-120	NE Marine and Ind	1	38.95	0	38.95	Vinyl Coated	Accessories
1/4" line	CO-01-040	NE Marine and Ind	400'	14.13	0	14.13	Sinking Line	Accessories
Construction Accessories	----	Various	----	----	0	31.94	bolts, screws, etc	Accessories
9/32" line		NE Marine and Ind	400'	18.01	0	18.01	floating line	Accessories
Tap	83755A45	McMaster-Carr Su	1	13.75	5	18.75	1/4" by 20	Accessories
					TOTAL	**971.09**		

References:

Atlantic Large Whale Take Reduction Plan, Federal Register: April 7, 1997, Vol. 62, No. 66.

Kraus, S.D. Rates and potential causes of mortality in North America right whales (Eubalaena glacialis). Mar. Mamm. Sci. 6(4): 278-291. 1990.

Hoerner, Sighard. Fluid - Dynamic Drag. Hoerner; Brick Town: 1965.

McDonald, Alan and Fox, Robert. Introduction to Fluid Dynamics. John Wiley and Sons, Inc; New York: 1992.

MMPA. Marine Mammal Protection Act. Library of Congress; Washington, DC: 1996.